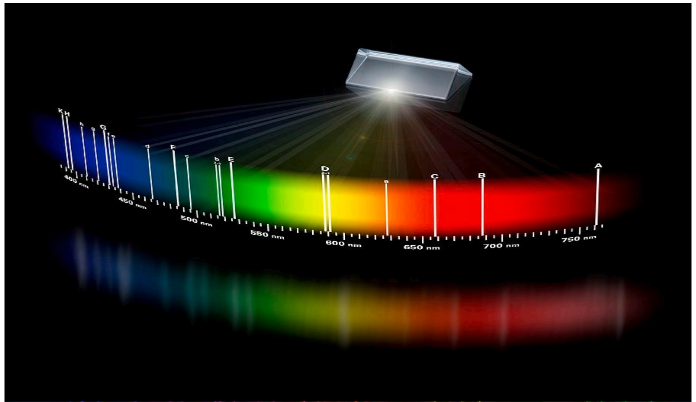

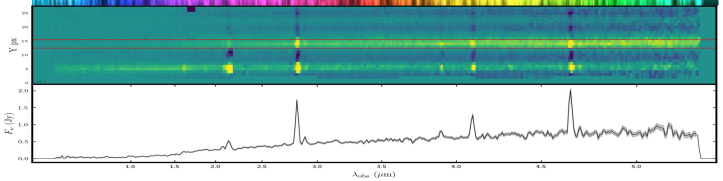

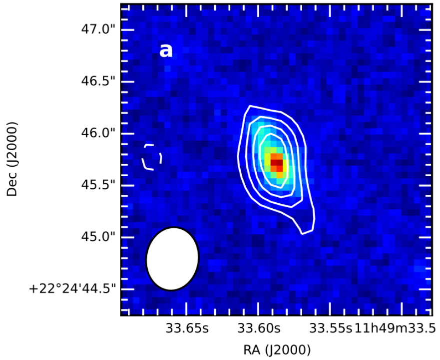

Best model for A1689z1 at z = 7.5. Reduced χ^2=1.41

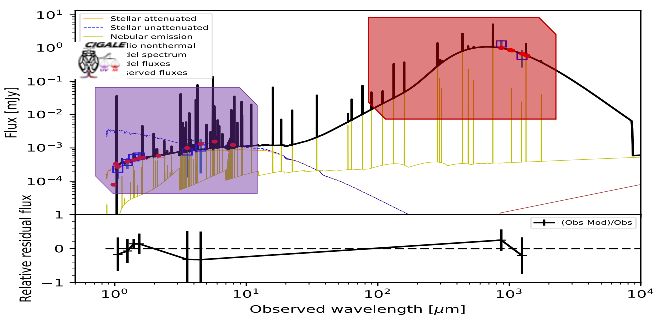

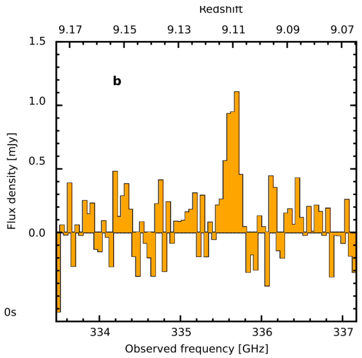

Identification of large-EW DSFGs from submm colours
&
Spectroscopic observations of DSFGs with JWST

Denis Burgarella
(LAM / AMU, France)

OBJECTIVE OF THIS WORK:
THE RISE OF METALS AND DUST IN THE EARLY UNIVERSE

The Life Cycle of Dust Grains *outside* & *inside* Galaxies

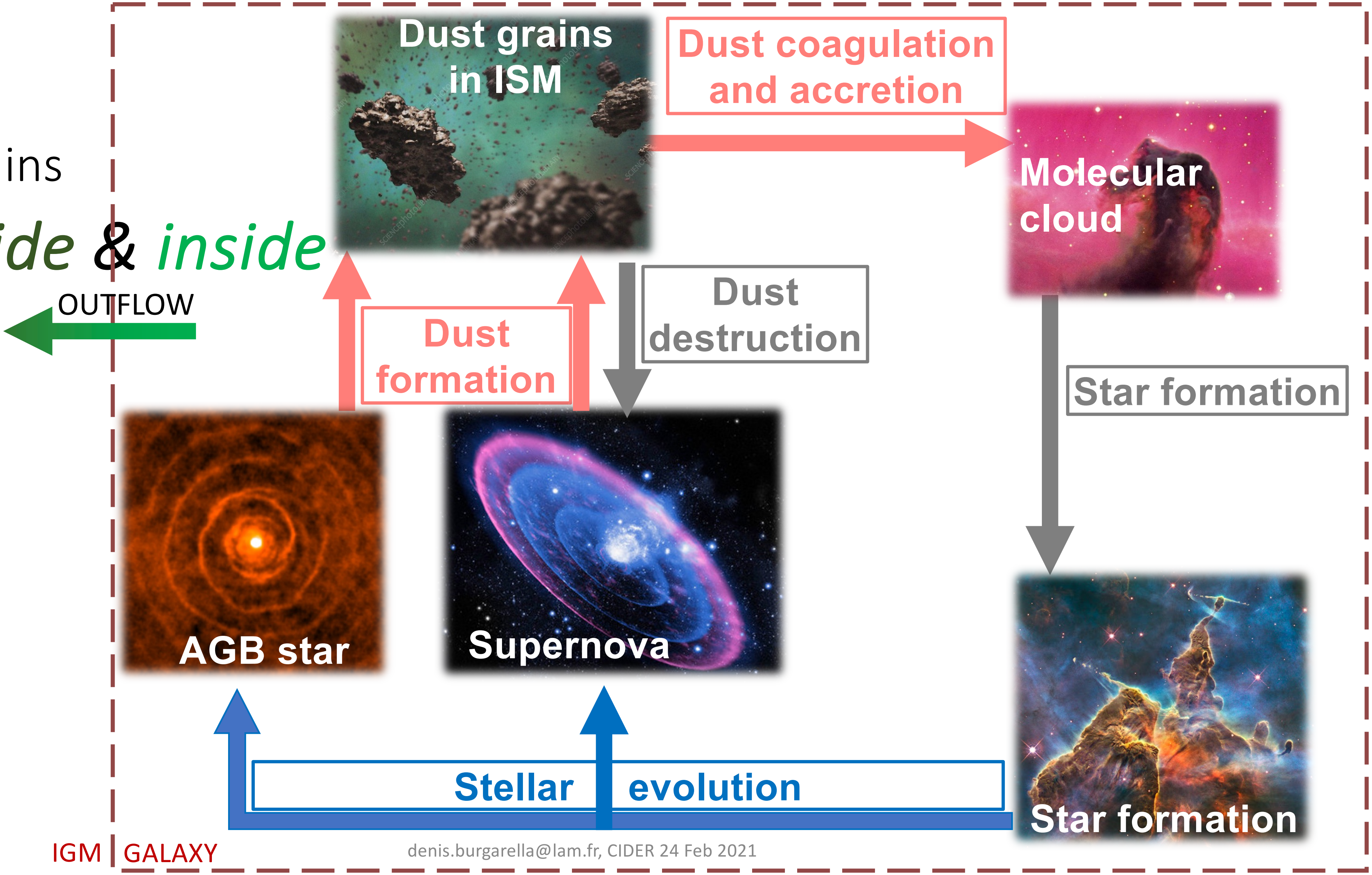

1. How to form so much dust in the early universe?

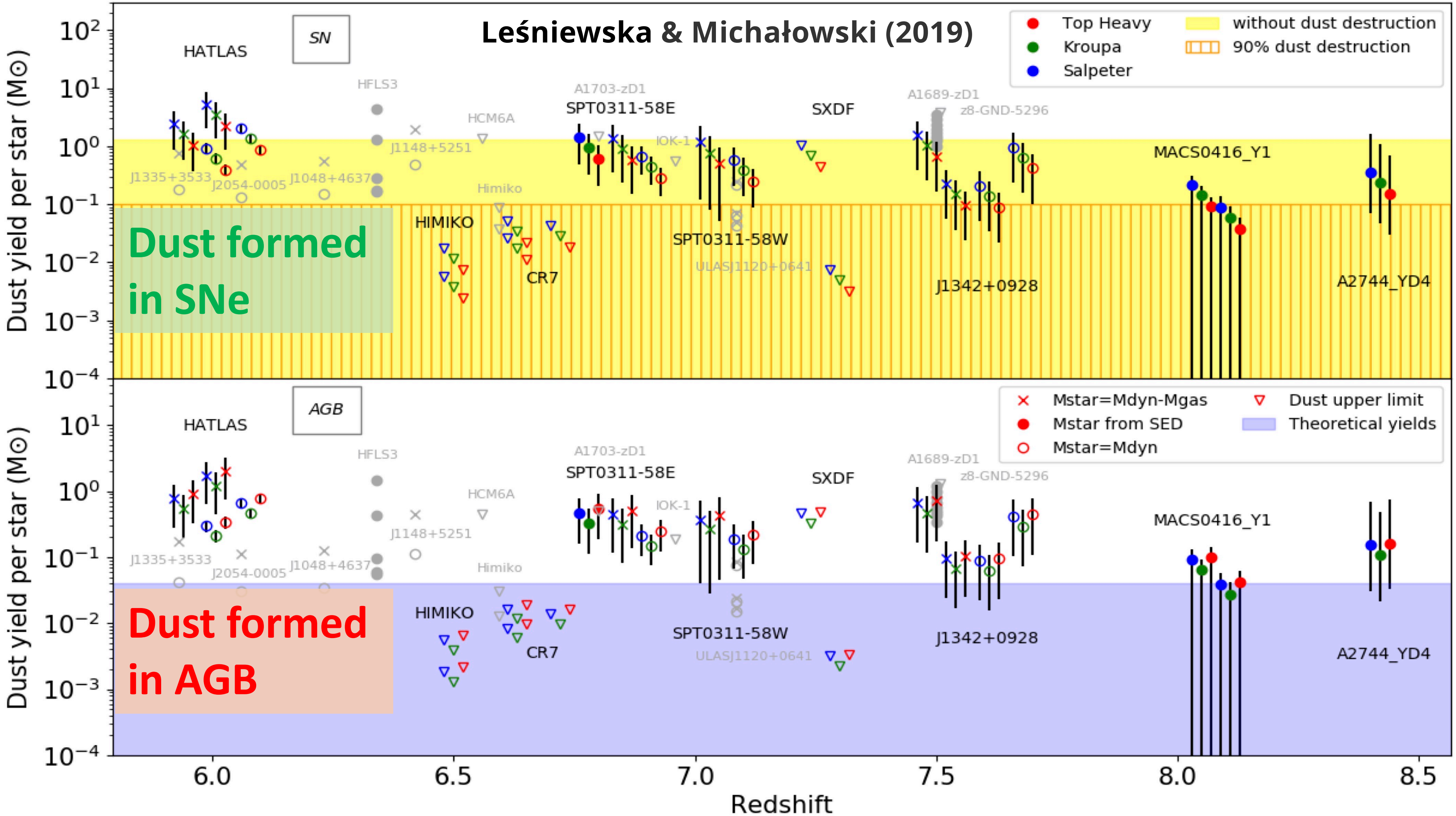

1. How to form so much dust in the early universe?

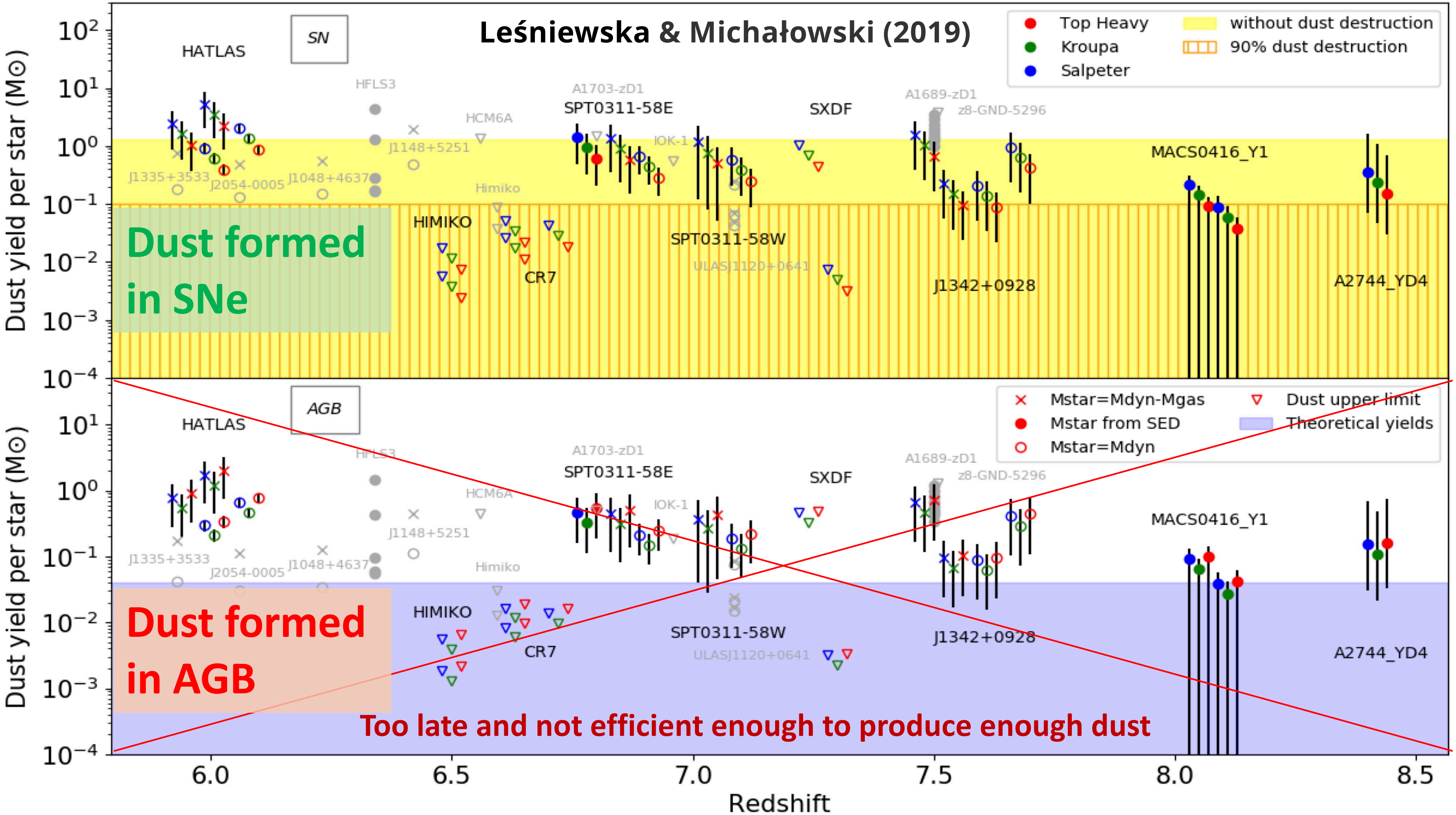

1. How to form so much dust in the early universe?

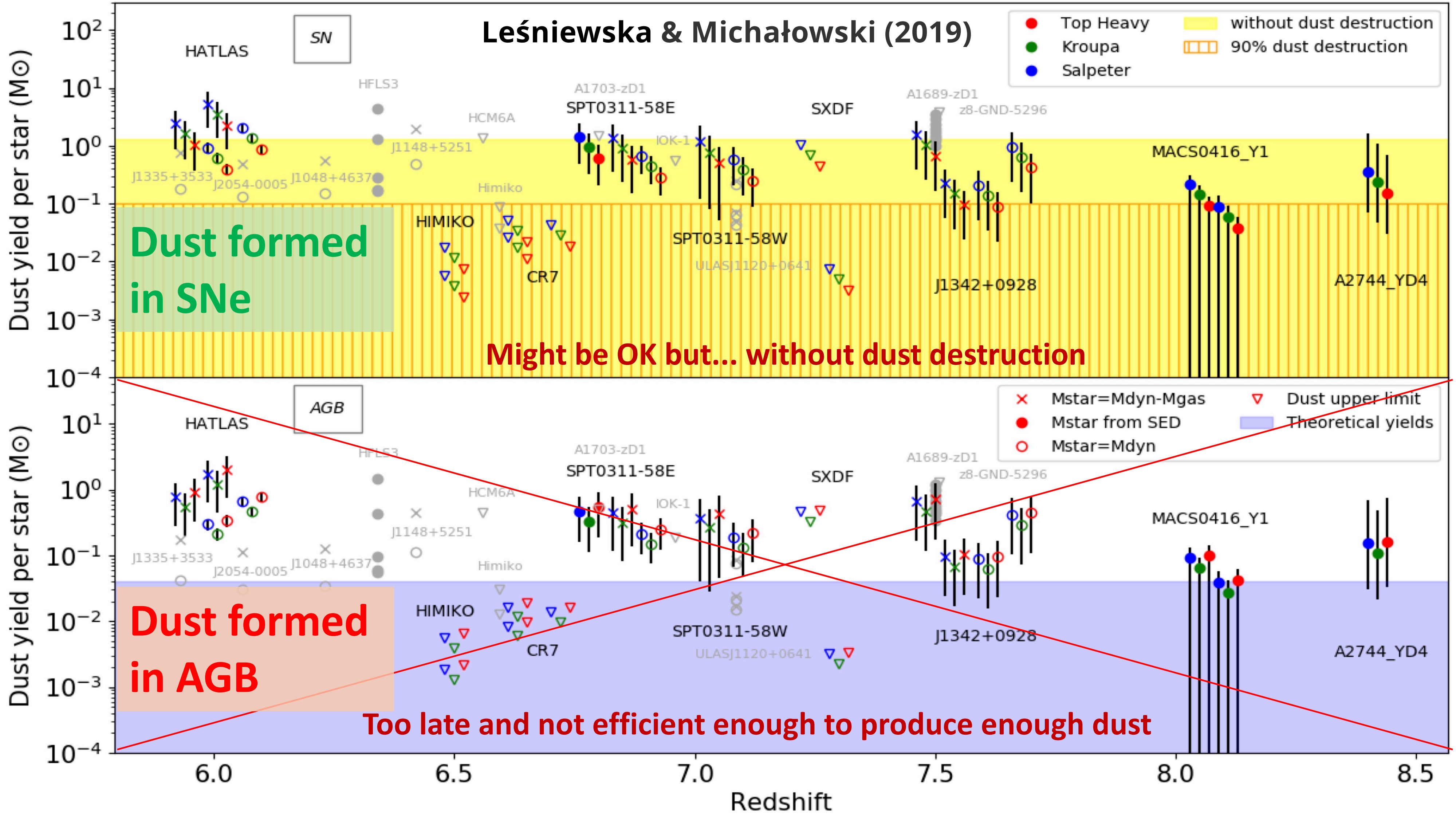

But we still are not sure about the dust cycle and how much dust is destroyed or rebuilt....

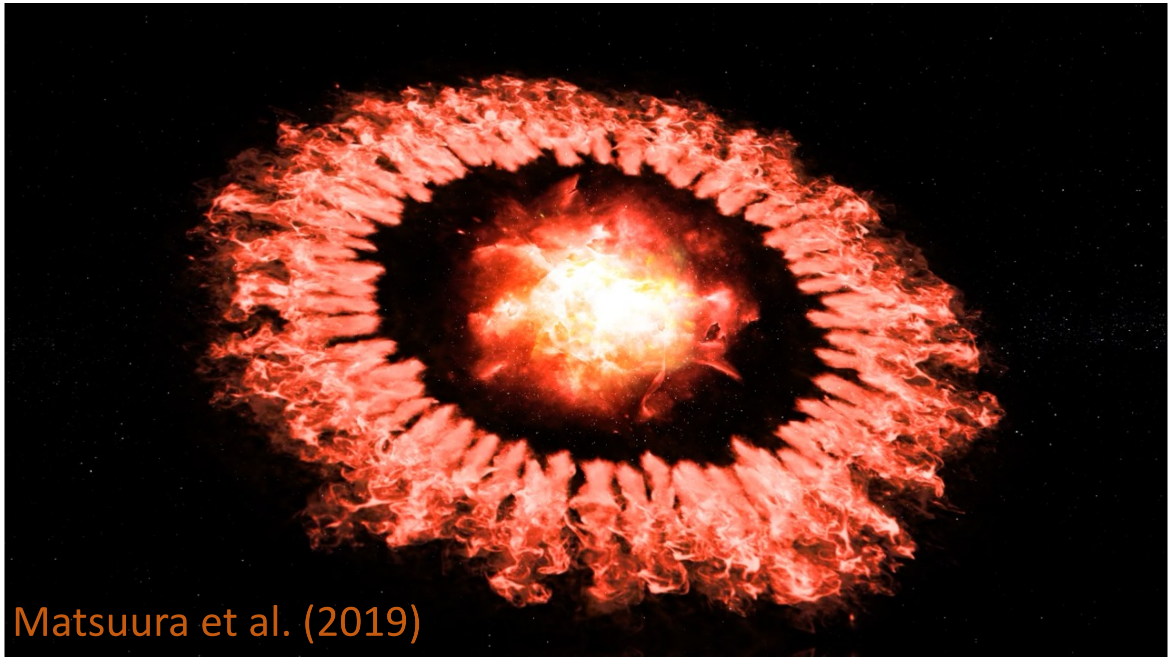

Artist's concept illustrating Supernova 1987A as the powerful blast wave passes through its outer ring and destroys most of its dust, before the dust re-forms or grows rapidly. SOFIA observations reveal that this dust — which make up the building blocks of stars and planets — can re-form or grow immediately after the catastrophic damage caused by the supernova's blast wave.
Credits: NASA/SOFIA/Symbolic Pictures/The Casadonte Group

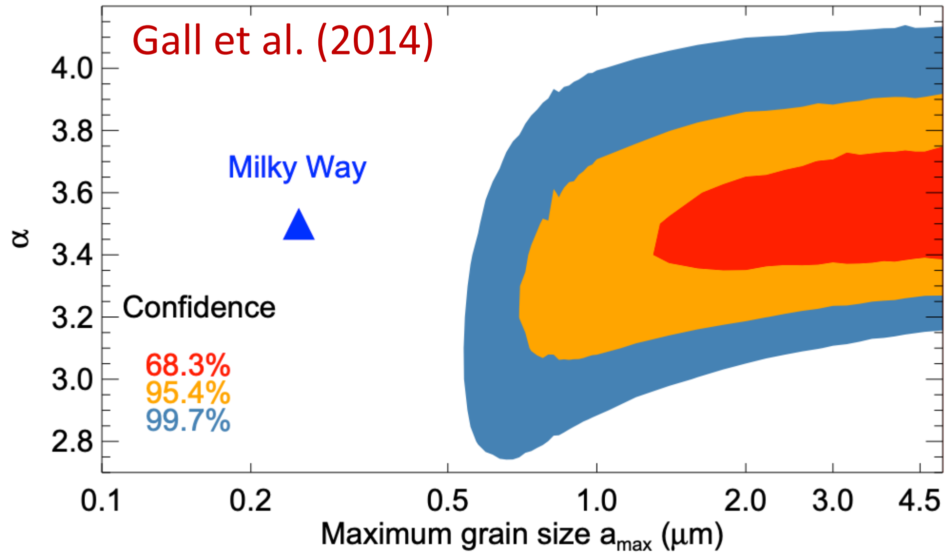

The wavelength dependent extinction of this dust reveals the presence of very large (> 1 μm) grains, which are resistant to destructive processes.

- Dust absorbs and re-emits light from (young) stars
- It gives access to the « obscured » star formation
- Dust obscured star formation peaks at z = 2-2.5 and has dominated the star formation back to z ~ 4
- At z ~ 6-7 it still represents ~25% of the total star formation

Zavala+21, MORA/ ALMA survey

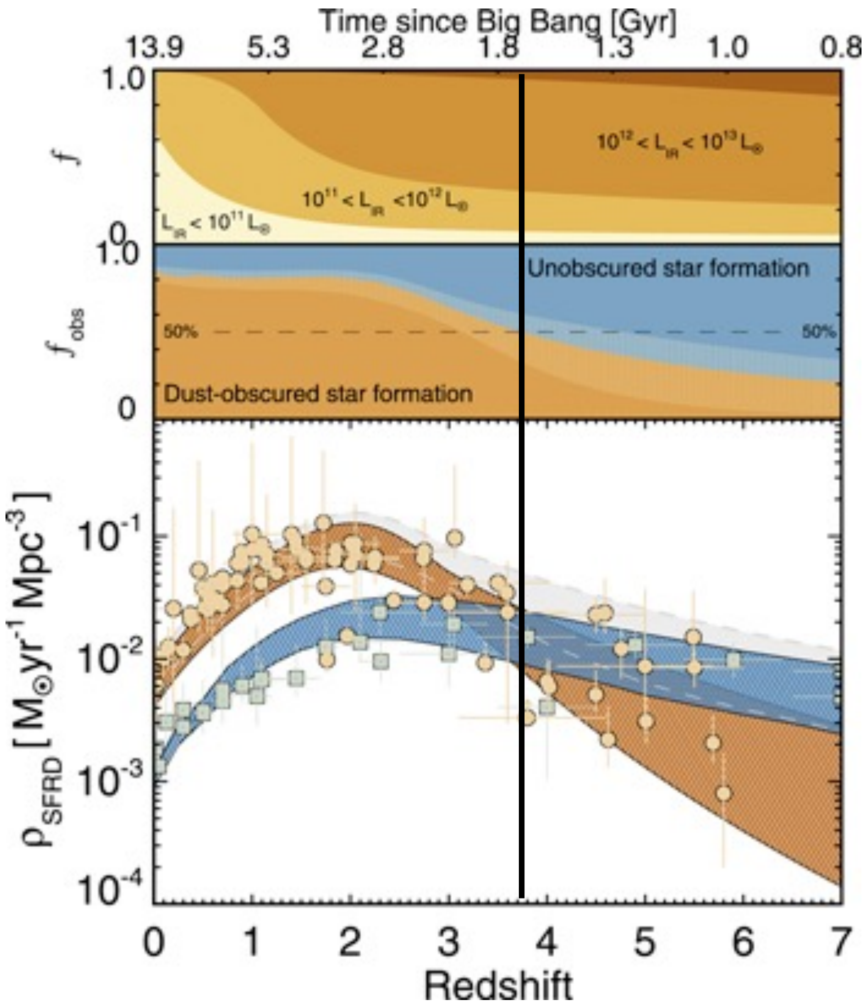

2023A&A...671A.123B

Identification of Large Equivalent Width Dusty Galaxies at 4 < z < 6 from Sub-mm Colours

D. Burgarella[1], P. Theulé[1], V. Buat[1], L. Gouiran[1] L. Turco[1] M. Boquien[2], T. J. L. C. Bakx[3,4], A. K. Inoue[5,6], Y. Fudamoto[4], Y. Sugahara[4,6], and J. Zavala[4]

[1] Aix Marseille Univ, CNRS, CNES, LAM, Marseille, France
e-mail: denis.burgarella@lam.fr
[2] Centro de Astronomía (CITEVA), Universidad de Antofagasta, Avenida Angamos 601, Antofagasta, Chile
[3] Division of Particle and Astrophysical Science, Graduate School of Science, Nagoya University, Aichi 464-8602, Japan
[4] National Astronomical Observatory of Japan, 2-21-1, Osawa, Mitaka, Tokyo 181-8588, Japan
[5] Department of Physics, School of Advanced Science and Engineering, Faculty of Science and Engineering, Waseda University, 3-4-1, Okubo, Shinjuku, Tokyo 169-8555
[6] Waseda Research Institute for Science and Engineering, Faculty of Science and Engineering, Waseda University, 3-4-1, Okubo, Shinjuku, Tokyo 169-8555

EXCESSES IN THE FLUX DENSITIES OF HIGH-REDSHIFT GALAXIES IN BROAD BANDS.

- Several papers suggest that there is a boost of the IRAC bands at z ~ 7 - 8 when Hα, and [OIII]500.7 nm fall in the mid-IR filters (Roberts-Borsani et al. 2016, 2020, de Barros et al. 2013, Anders et al. 2003)

- In the far-IR, Smail et al. 2011 estimated that 1 % of the bolometric emission of the [CII]158 um fine structure line would boost the broad band flux densities by ~ 20 - 40 %.
- Seymour et al. (2012) as well, explain the excess in the SPIRE 500 um by the contribution of [CII]158 um

Excesses in the flux densities of high-redshift galaxies in broad bands.

ROBERTS-BORSANI ET AL.

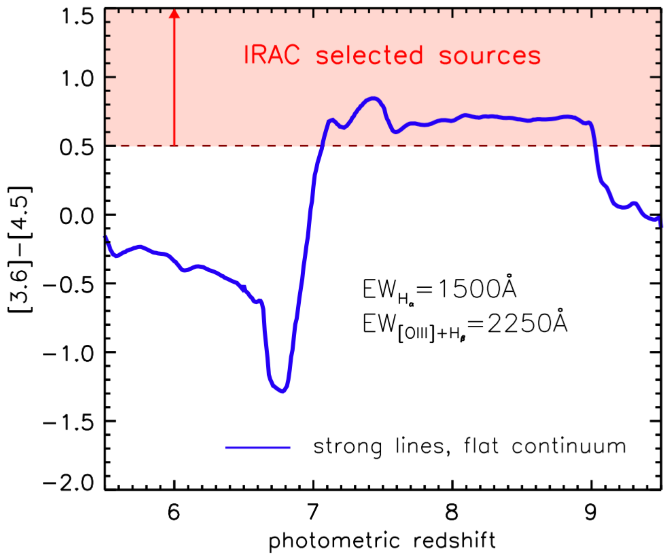

Figure 1. *Spitzer*/IRAC [3.6]−[4.5] color vs. photometric redshift plot for young (∼5 Myr) stellar populations with very strong nebular emission lines ($EW_{H\alpha}$ = 1500 Å) and a flat continuum. Also assumed are fixed flux ratios between emission lines from Table 1 of Anders & Fritze-v. Alvensleben (2003) for 0.2 $Z_\odot$ metallicity, while assuming case B recombination for the $H\alpha/H\beta$ flux ratio. The [3.6]–[4.5] color of galaxies is expected to become quite red at $z \gtrsim 7$ due to the impact of the [O III] line on the 4.5 μm band and no comparably bright nebular line in the 3.6 μm.

Roberts-Borsani et al. 2016

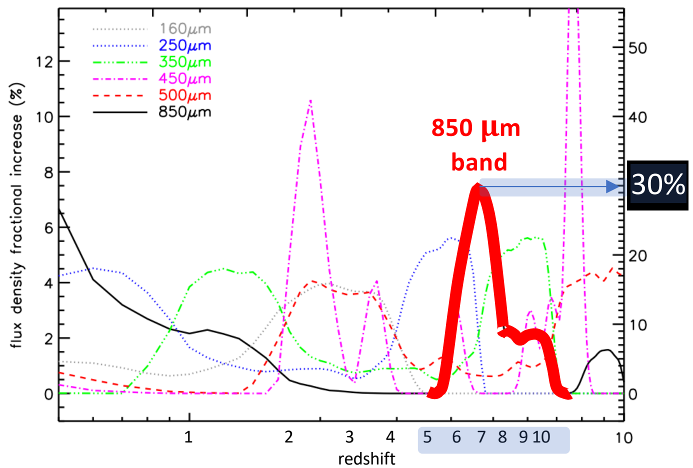

Fig. 3 — The contribution as a function of source redshift to the continuum emission in the *Herschel* PACS and SPIRE, SCUBA-2 and LABOCA bands, from the emission lines shown in Fig. 2. The influence of the [CII] 158μm line can be seen in the 250-, 350-, 500- and 850-μm bands at $z \sim 0.6$, 1.2, 2.2 and 4.4 respectively with a contribution to the broad-band fluxes of 5–10%. Note that these contributions are based on a [CII] line comprising 0.27% of the galaxy's L_{FIR}. The line contributions will scale linearly with the line to far-infrared luminosity ratio, so sources with $L_{[CII]}/L_{FIR} \gtrsim 1\%$ (Fig. 1) will have contributions $\gtrsim 4\times$ larger, $\sim$ 20–40%, corresponding to the right-hand flux scale. We caution that the contributions for the higher redshift sources in the shorter wavelength filters (e.g. at $z \sim 4$ and $z \sim 6$ at 250 and 350μm respectively) are based on predicted, rather than observed, line fluxes.

Smail et al. 2011

The SPT galaxy sample

Reuter et al. (2020) presented the final spectroscopic redshift analysis of a flux-limited ($S_{870\mu m}$ > 25 mJy) sample of galaxies from the 1.4 mm SPT survey.

In this 2500 square degree survey observed at 1.4mm and 2.0mm, they identified 81 strongly lensed, dusty star-forming galaxies (DSFGs) at $1.9<z<6.9$.

The spectroscopic observations were conducted with ALMA across the 3-mm spectral window, targeting carbon monoxide line emission.

The data themselves are from Reuter et al. (2020).

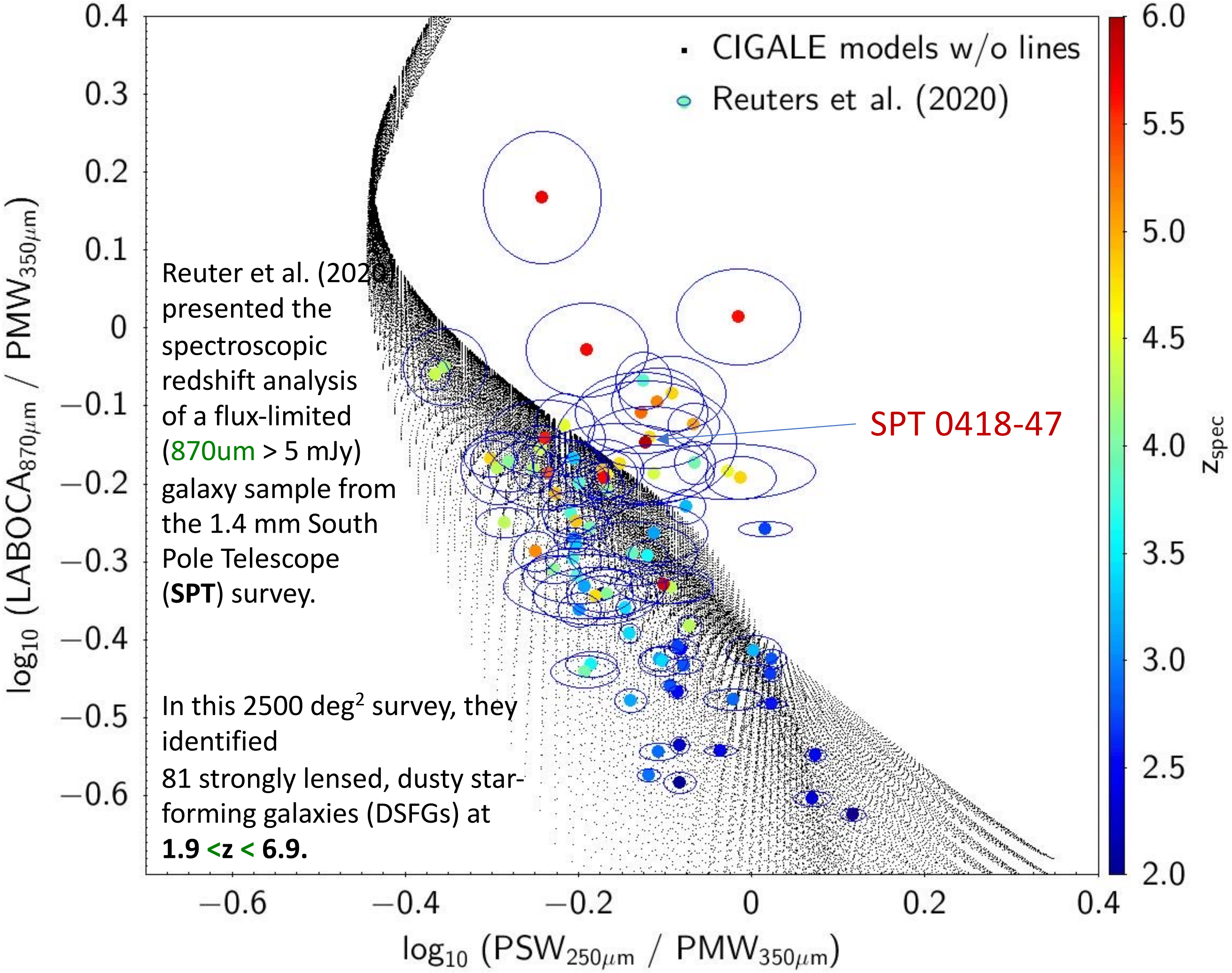

A colour-colour approach for the selection of galaxies at z > 4

1. No emission lines included in the SEDs
2. ~~Emission lines included into the SEDs~~

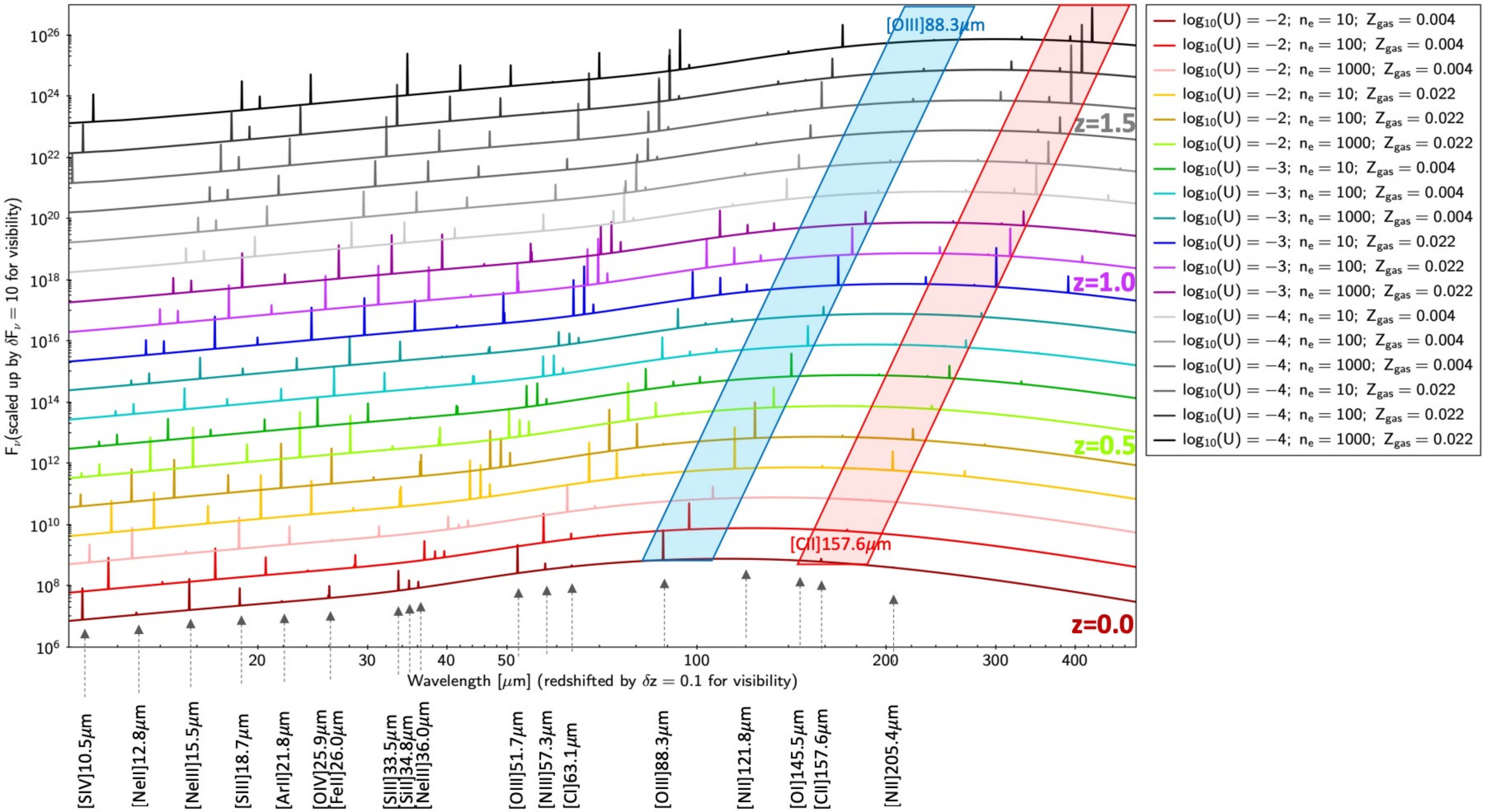

[OIII]88.3μm
[CII]157.6μm
z=1.5
z=1.0
z=0.5
z=0.0
F_ν(scaled up by $\delta F_\nu = 10$ for visibility)
Wavelength [μm] (redshifted by $\delta z = 0.1$ for visibility)
$\log_{10}(U) = -2;\ n_e = 10;\ Z_{gas} = 0.004$
$\log_{10}(U) = -2;\ n_e = 100;\ Z_{gas} = 0.004$
$\log_{10}(U) = -2;\ n_e = 1000;\ Z_{gas} = 0.004$
$\log_{10}(U) = -2;\ n_e = 10;\ Z_{gas} = 0.022$
$\log_{10}(U) = -2;\ n_e = 100;\ Z_{gas} = 0.022$
$\log_{10}(U) = -2;\ n_e = 1000;\ Z_{gas} = 0.022$
$\log_{10}(U) = -3;\ n_e = 10;\ Z_{gas} = 0.004$
$\log_{10}(U) = -3;\ n_e = 100;\ Z_{gas} = 0.004$
$\log_{10}(U) = -3;\ n_e = 1000;\ Z_{gas} = 0.004$
$\log_{10}(U) = -3;\ n_e = 10;\ Z_{gas} = 0.022$
$\log_{10}(U) = -3;\ n_e = 100;\ Z_{gas} = 0.022$
$\log_{10}(U) = -3;\ n_e = 1000;\ Z_{gas} = 0.022$
$\log_{10}(U) = -4;\ n_e = 10;\ Z_{gas} = 0.004$
$\log_{10}(U) = -4;\ n_e = 100;\ Z_{gas} = 0.004$
$\log_{10}(U) = -4;\ n_e = 1000;\ Z_{gas} = 0.004$
$\log_{10}(U) = -4;\ n_e = 10;\ Z_{gas} = 0.022$
$\log_{10}(U) = -4;\ n_e = 100;\ Z_{gas} = 0.022$
$\log_{10}(U) = -4;\ n_e = 1000;\ Z_{gas} = 0.022$
[SIV]10.5μm
[NeII]12.8μm
[NeIII]15.5μm
[SIII]18.7μm
[ArII]21.8μm
[OIV]25.9μm
[FeII]26.0μm
[SIII]33.5μm
[SiII]34.8μm
[NeIII]36.0μm
[OIII]51.7μm
[NIII]57.3μm
[CI]63.1μm
[OIII]88.3μm
[NII]121.8μm
[OI]145.5μm
[CII]157.6μm
[NII]205.4μm

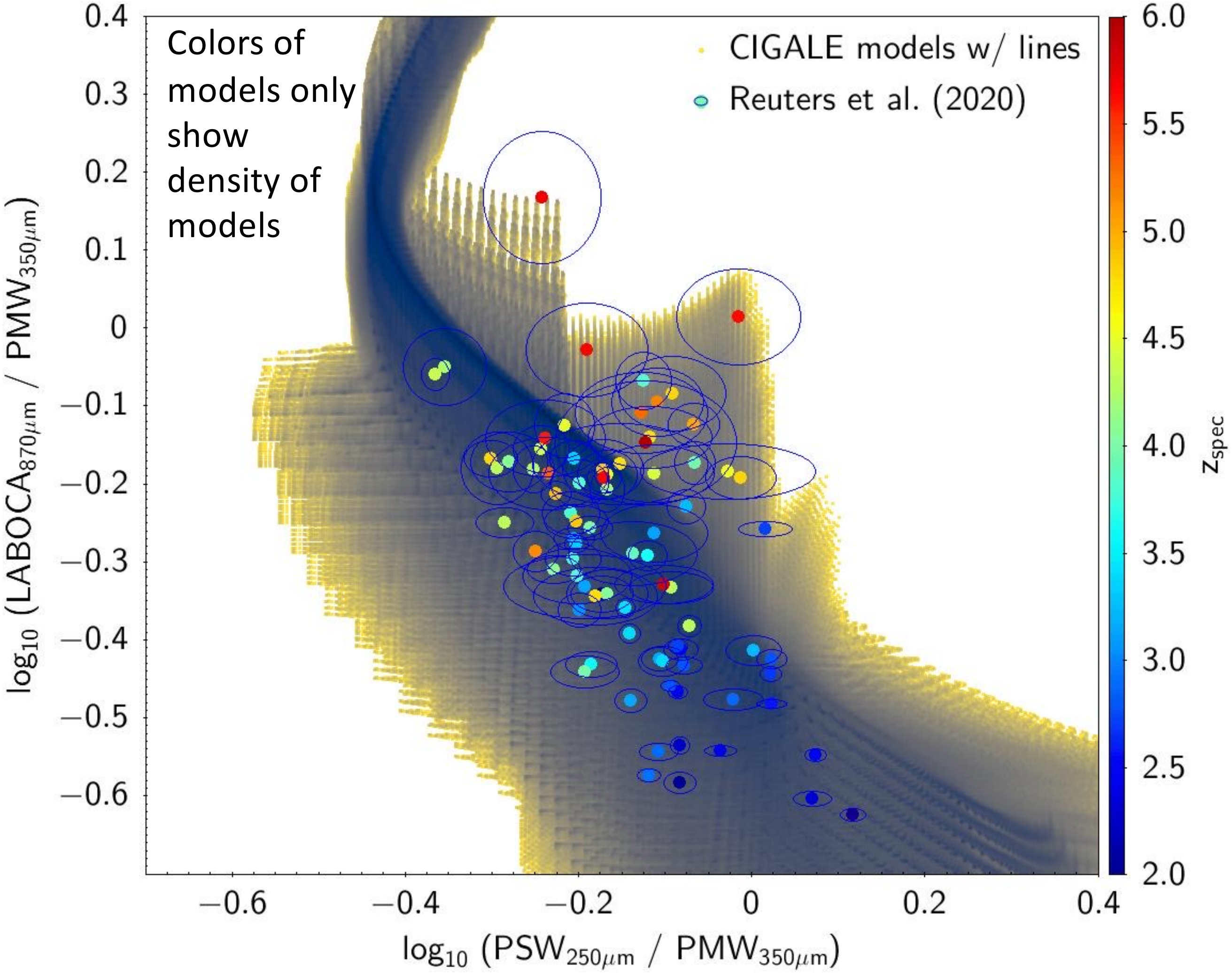

A colour-colour approach for the selection of galaxies at z > 4

1. ~~No emission lines included in the SEDs~~
2. Emission lines included into the SEDs

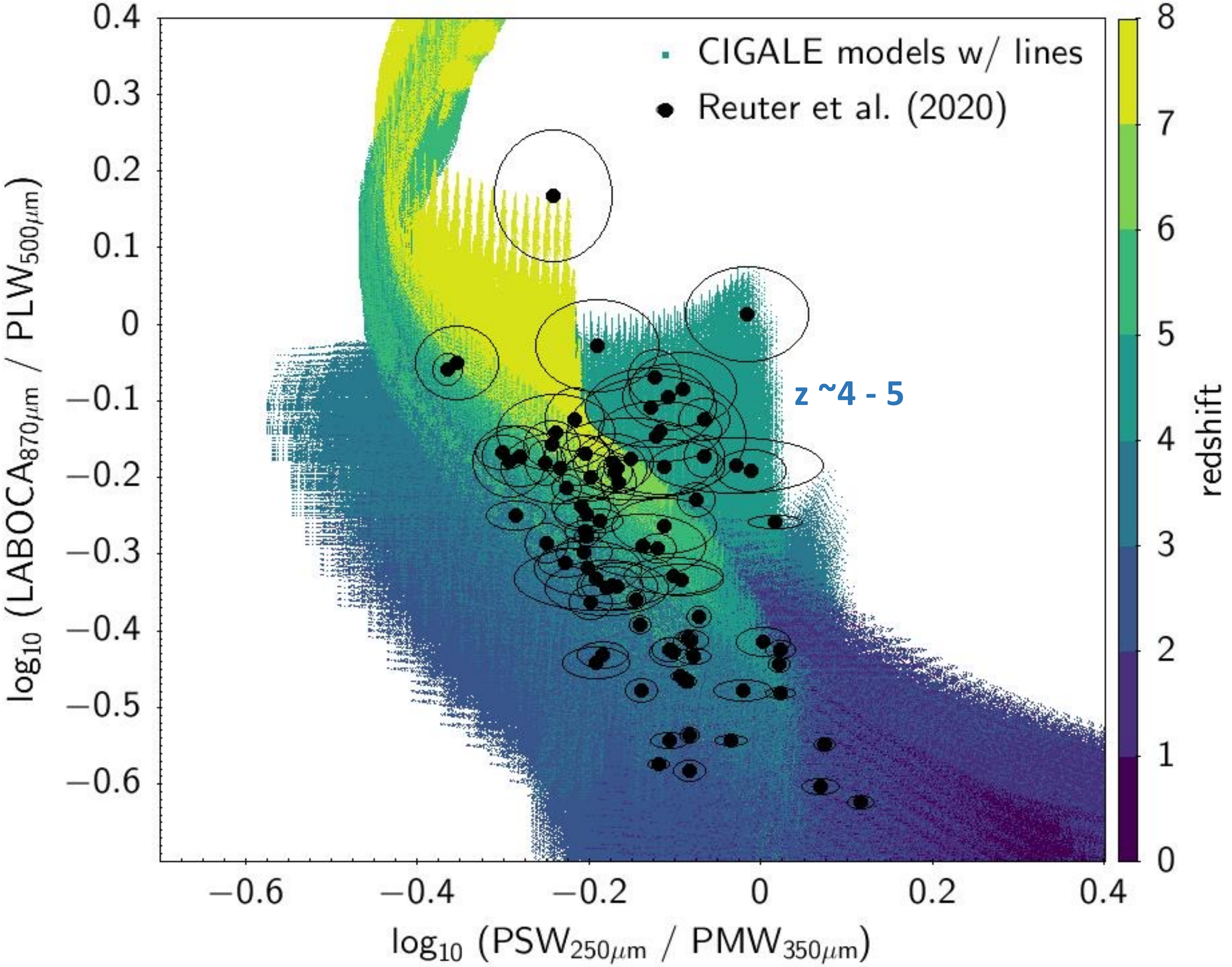

A colour-colour approach for the selection of galaxies at z > 4

1. ~~No emission lines included in the SEDs~~
2. Emission lines included into the SEDs

Which line(s) explain(s) this effect?

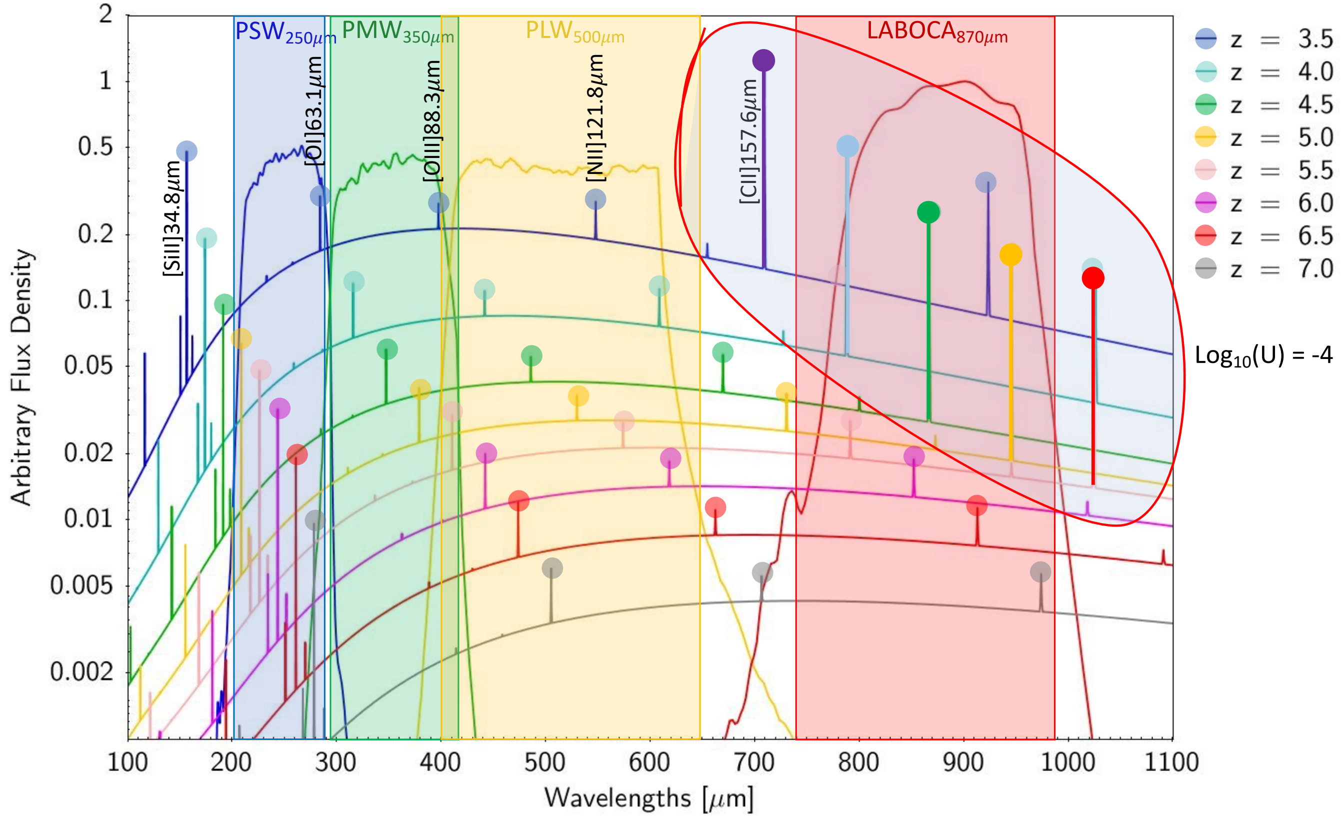

For this sample of SPT galaxies, **[CII]158 um** is at the origin of the outliers

Which line(s) explain(s) this effect?

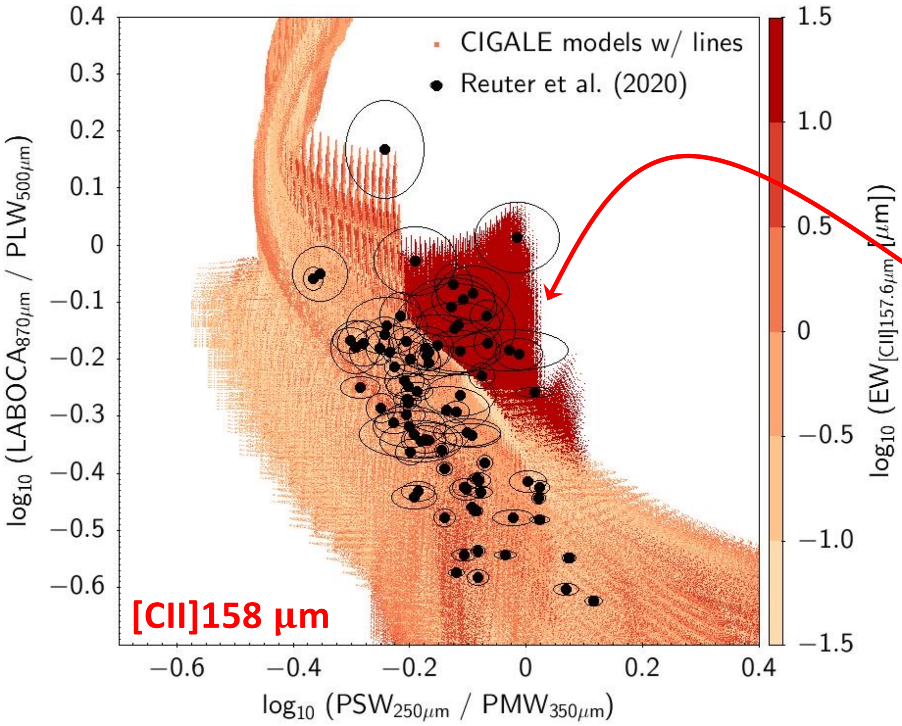

For this sample of SPT galaxies, **[CII]158 um** is at the origin of the outliers

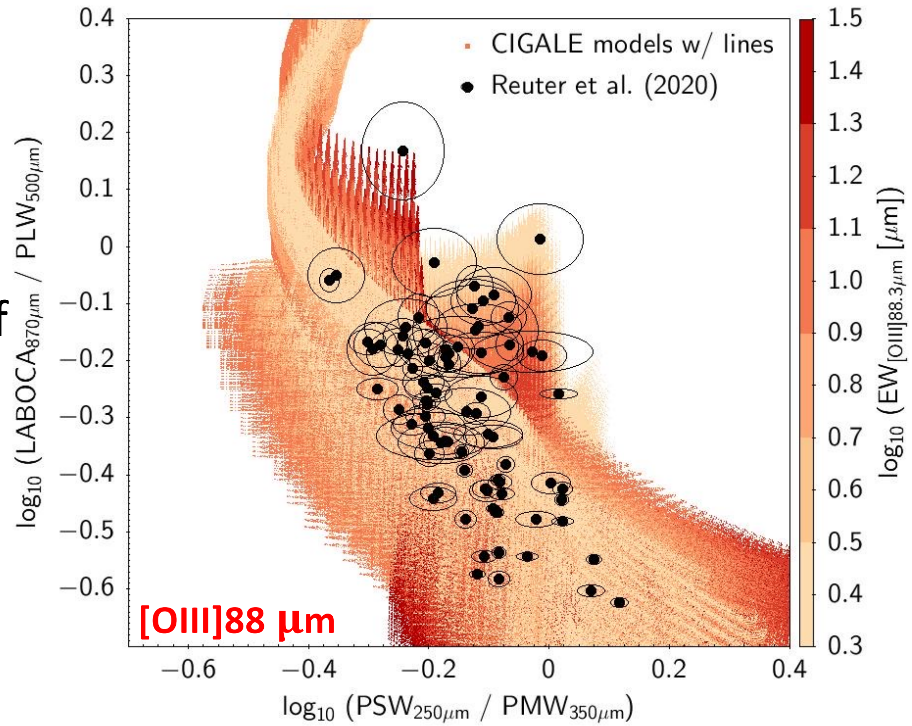

The derived distribution in the $\log_{10}$ (U) vs. Z diagramme

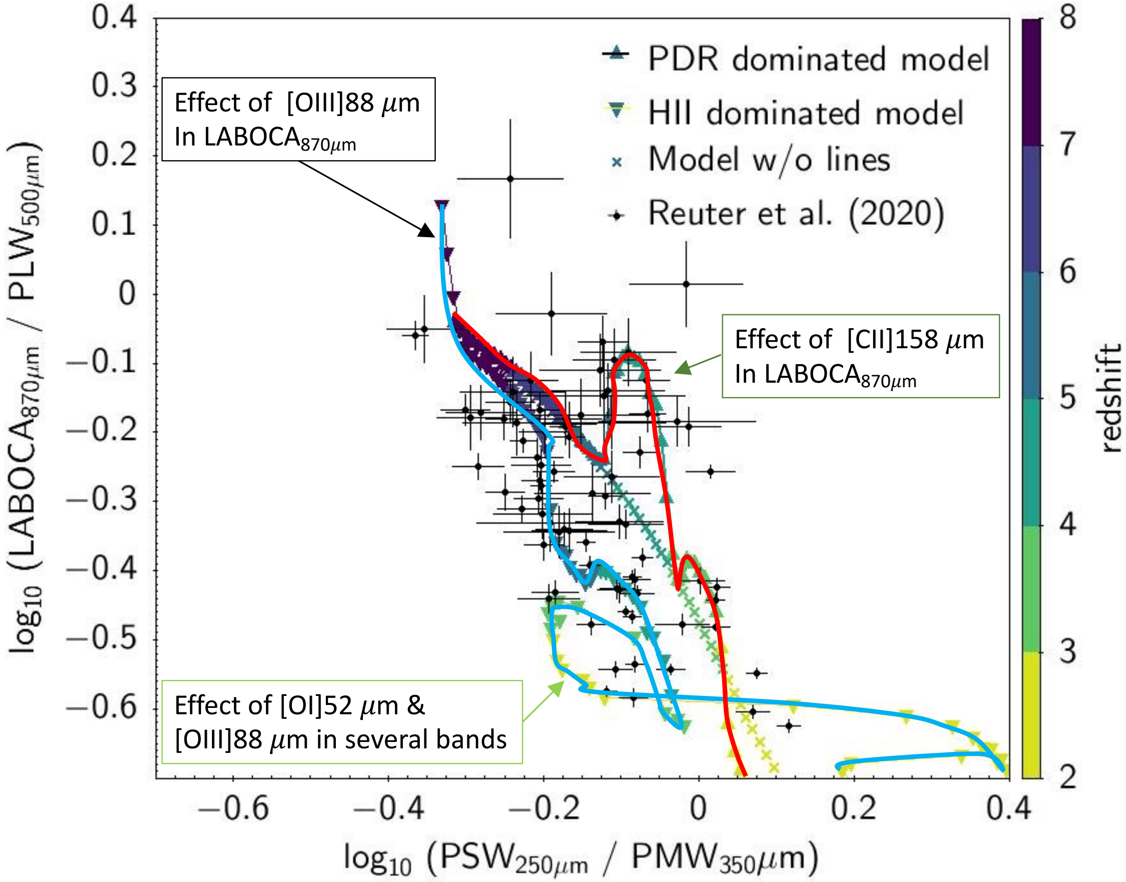

At log10 (U) = -4.0, the strong [CII]157.6 um line induces an upward move of $\log_{10}$ ($LABOCA_{870um}$ / PLW_{500um}) that corresponds to the clump of high redshift galaxies.

However, even though the move of the [OIII]51.8 um and [OIII]88.3 um lines of galaxies with a strong emission from HII regions at log10 (U) = -2.0 could induce specific colours, the effect is less clear as models with no lines can also lie here.

A New Vision of the Epoch of Reionization, and the Ultra-High Redshift Universe at z > 10

- In December 2022, the James Webb Space Telescope was launched.
- A few months after, new JWST data started to rain down on human astronomers.

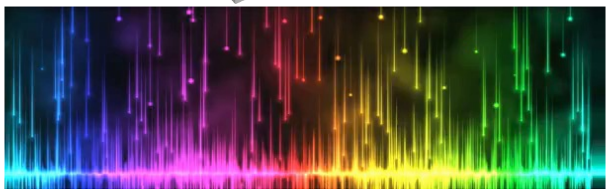

- Even though some teams apparently worked too fast and “identified” galaxies at $z = 15 - 20$, more serious works measured many photometric and later spectroscopic redshifts in the epoch of reionization, and even at $z > 10$.
- In our basked, we have now collected many galaxy spectra at all redshifts from various JWST programs (JADES, CEERS, GLASS).

A New Vision of the Epoch of Reionization, and the Ultra-High Redshift Universe at z > 10

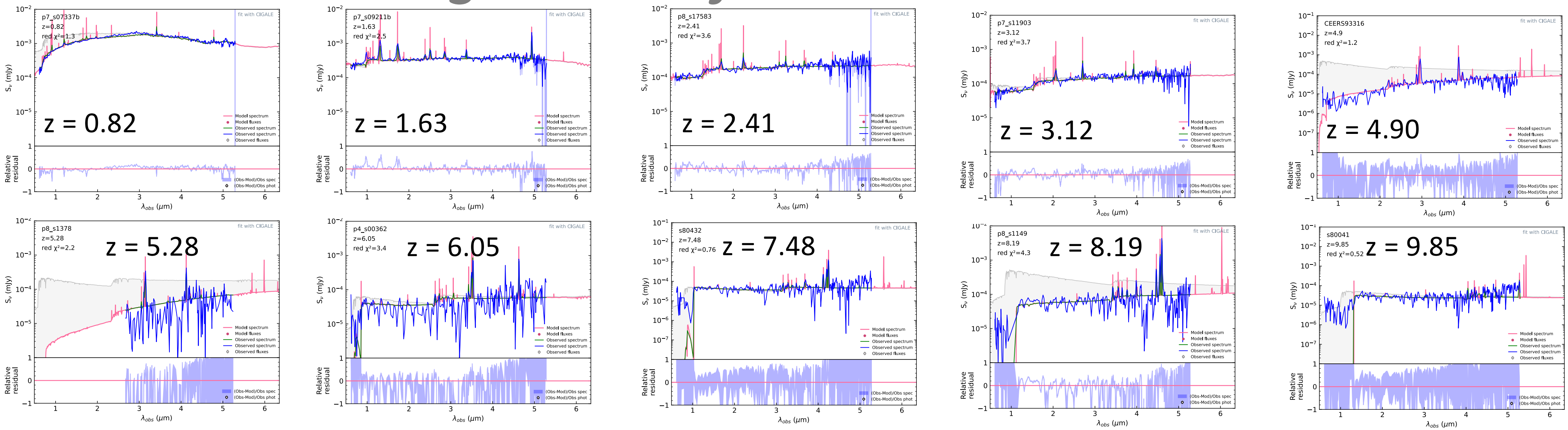

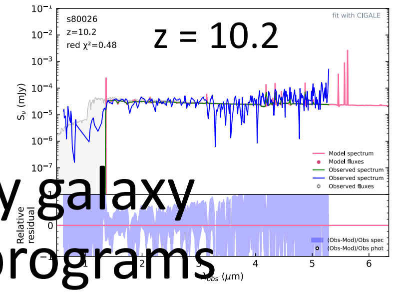

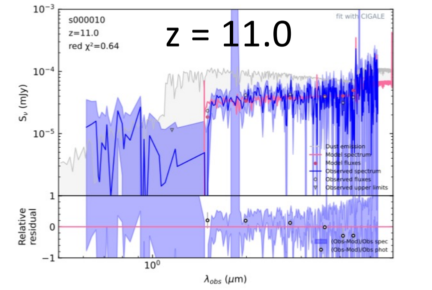

- In our basked, we have now collected many galaxy spectra at all redshifts from various JWST programs (JADES, CEERS, GLASS).

Lots of **NIRSpec information on high-z objects**

…we need to complement this information with millimeter observations (ALMA… and maybe NOEMA)

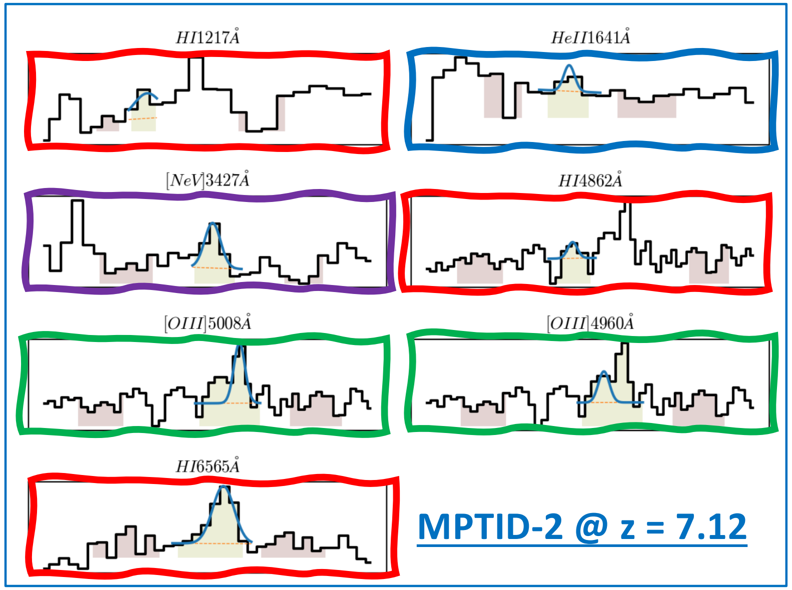

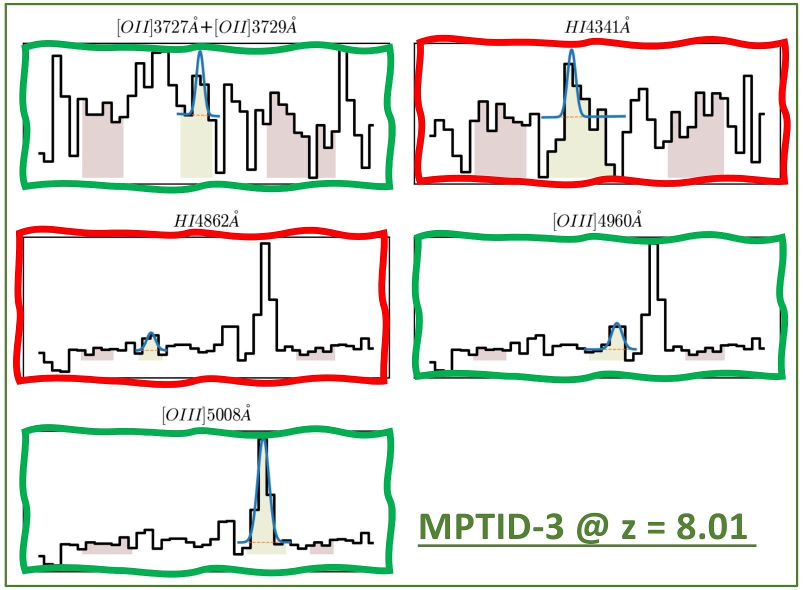

CEERS line profiles database by Vital Fernandez (Chile)

MPTID-3 and MPTID-2355 have M_{star} ~ 1 – 3 x 10^9 $M_\odot$ and MPTID-2 has M_{star} ~ 1.5 x 10^8 $M_\odot$

MPTID-1019 @ z = 8.68

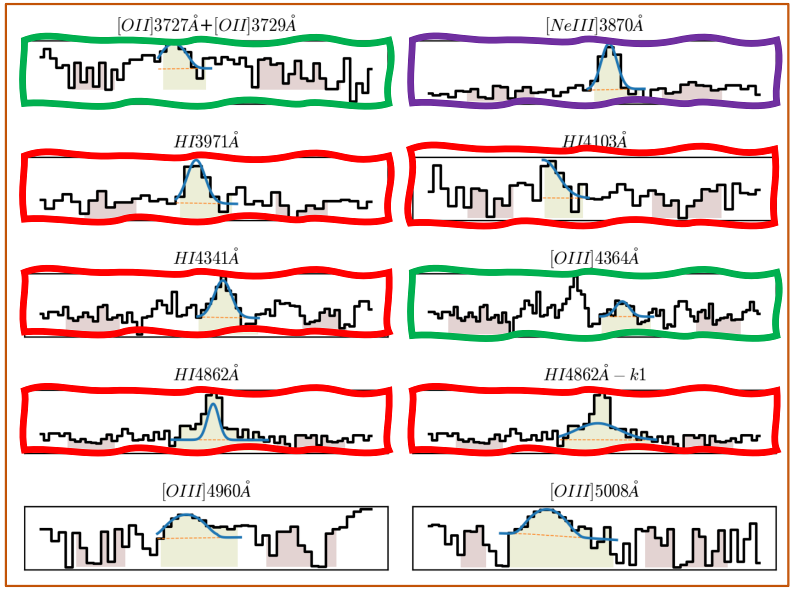

From NIRSpec:

- **Hydrogen lines**
- **Oxygen lines**
- **Helium line**
- **Ne lines**

From NOEMA:

- **Carbon line**
- **Dust continuum**

A New Vision of the Epoch of Reionization, and the Ultra-High Redshift Universe at z > 10

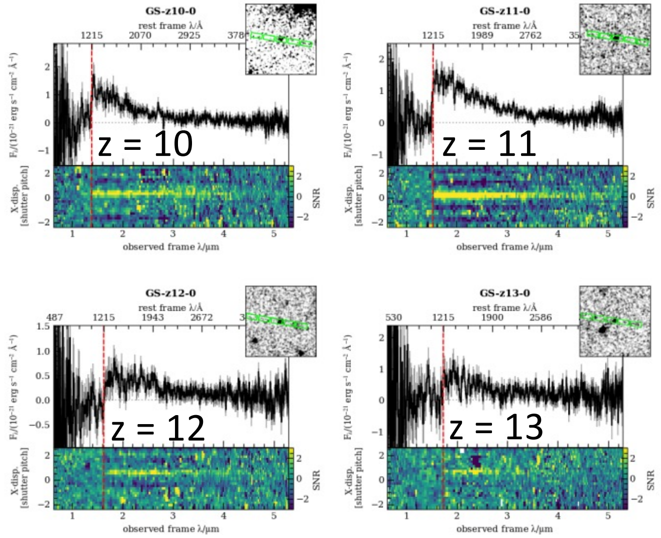

Fig. 1 NIRSpec prism $R \sim 100$ spectra for the four $z > 10$ galaxies targeted for the first deep spectroscopic pointing of the JADES survey, JADES-GS-z10-0, JADES-GS-z11-0, JADES-GS-z12-0 and JADES-GS-z13-0. For each galaxy we display the 1D spectrum and associated uncertainties. In the bottom panel we show the 2D signal-to-noise ratio plot. The 2D plot is binned over four pixels in the wavelength direction to better show the contrast across the break. The inset panel in the top right-hand corner shows the NIRCam F444W filter image with the three nodding positions of the the NIRSpec micro-shutter 3-slitlet array aperture shown in green. The red dashed line shows 1215.67Å at the observed redshift z_{1216}.

Curtis-Lake et al. (2023)

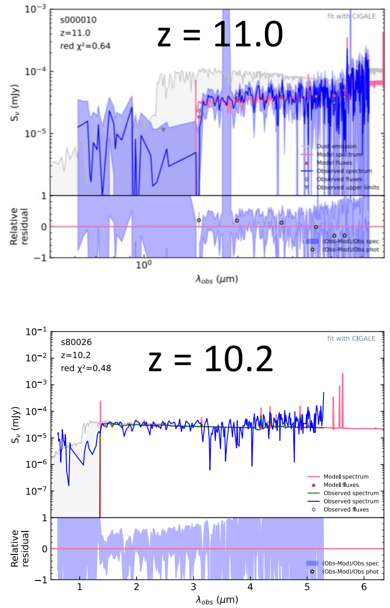

Burgarella et al. (2024, in prep.)

- In our basked, we have now collected many galaxy spectra at all redshifts from various JWST programs (JADES, CEERS, GLASS)… and even at $z_{spec} > 10$.

MSA-ID-10 galaxy (NIRCam F277W = 27.3 Abmag)

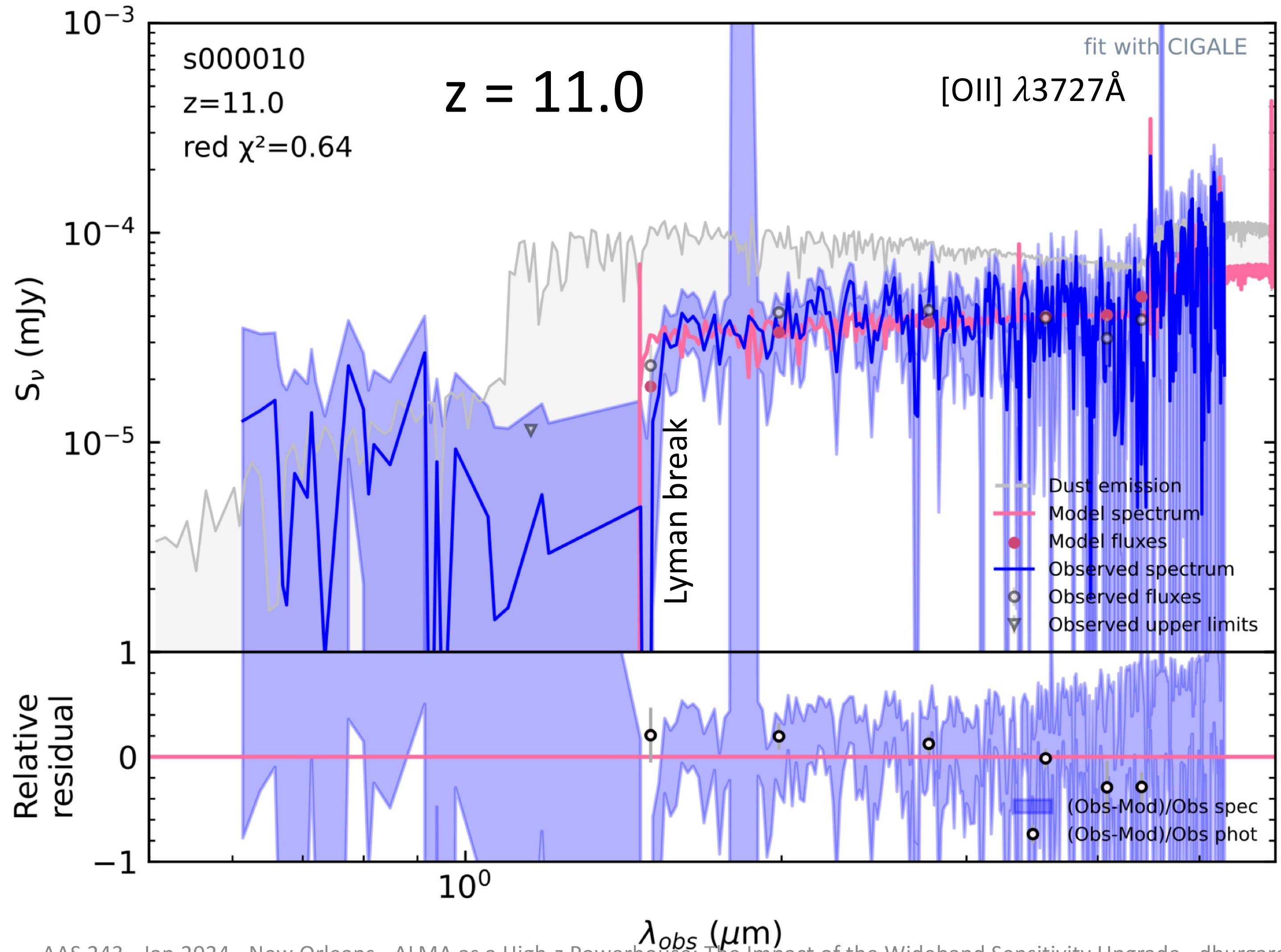

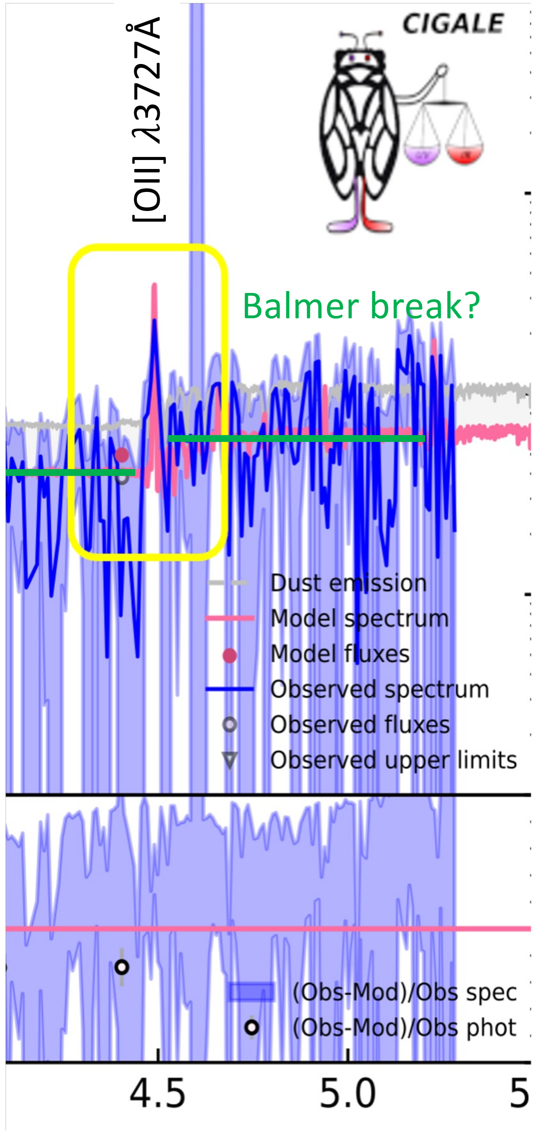

Maisie's galaxy (NIRCam F277W = 27.9 Abmag)

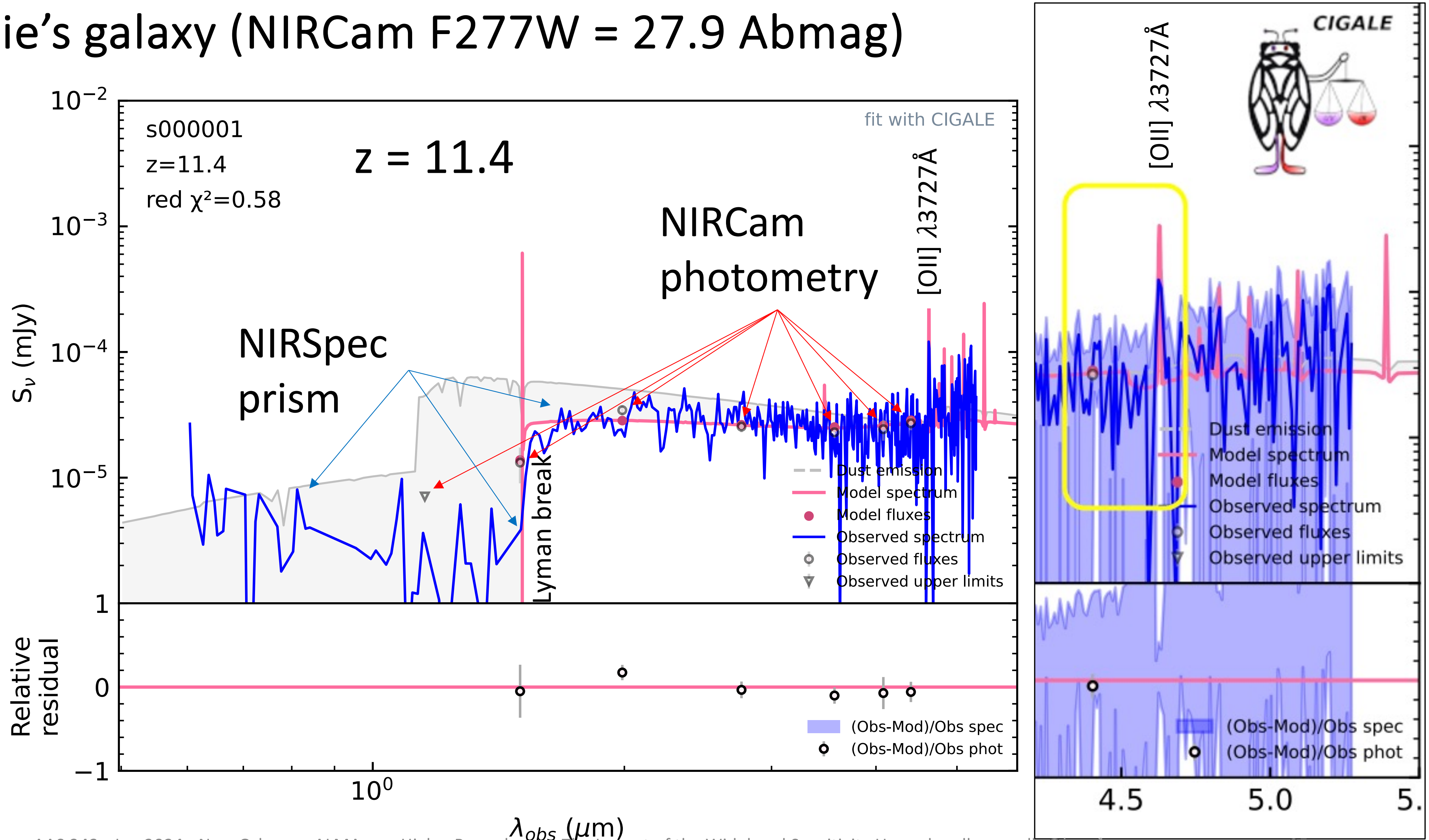

Fitting photometric, spectroscopic and equivalent widths / line fluxes

id	χ^2_ν	EW([OII]) nm	EW([OII])_err nm	EW(Hγ) nm	EW(Hγ)_err nm	EW([OIII]]) nm	EW([OIII]])_err nm	EW(Hβ) nm	EW(Hβ)_err nm	EW(Hα) nm	EW(Hα)_err nm	EW([SII]]) nm	EW([SII]])_err nm	
s000001_phot	0.161	5.021	7.745											Fit
s000001_photEW	0.174	5.976	7.929											
s000001_photspec	0.581	5.266	2.085											
s000001_photspecEW	0.581	5.427	2.091											
s000003_phot	0.403	1.234	2.289	3.011	1.116	102.473	34.164	11.821	3.806	66.590	20.024	3.014	1.625	Fit
s000003_photEW	4.909	7.069	0.325	3.070	0.079	99.732	1.050	12.221	0.150	72.462	2.292	5.338	0.195	
s000003_photspec	0.798	4.335	1.587	2.757	0.216	95.887	7.093	10.943	0.689	62.827	3.851	3.942	0.720	
s000003_photspecEW	0.932	7.267	0.256	3.097	0.073	99.393	1.046	12.212	0.148	70.436	1.916	5.173	0.156	
s000010_phot	0.153	2.570	5.512											Fit
s000010_photEW	0.163	2.614	1.366											
s000010_photspec	0.639	3.415	1.271											
s000010_photspecEW	0.638	3.412	0.852											
id	Observed EWs:	EW([OII])	EW([OII])_err	EW(Hγ)	EW(Hγ)_err	EW([OIII]])	EW([OIII]])_err	EW(Hβ)	EW(Hβ)_err	EW(Hα)	EW(Hα)_err	EW([SII]])	EW([SII]])_err	Measured
s000001		2.700	19.300											
s000003		12.900	1.200	5.700	1.600	99.900	1.200	11.500	0.300	75.400	6.500	9.200	0.800	
s000010		3.300	1.400											

Object	z	$M/M_\odot$
s000001	11.4	$(4.96 \pm 3.52)\ 10^8$
s000003	4.9	$(9.96 \pm 3.61)\ 10^8$
s000010	11.0	$(1.85 \pm 0.66)\ 10^9$

- EWs used in addition to photometric data help a lot to derive the physical parameters
- Fitting spectroscopic data provides a good alternative to measuring EWs or line fluxes

Fitting photometric, spectroscopic and equivalent widths / line fluxes

id	χ^2_ν	M_{star} [$M_\odot$]	M_{star_err} [$M_\odot$]	SFR_{10Myrs} [$M_\odot yr^{-1}$]	SFR_{10Myrs_err} [$M_\odot yr^{-1}$]	A_V [$M_\odot yr^{-1}$]	A_{V_err} [$M_\odot yr^{-1}$]	age_{main} [Myr]	age_{main_err} [Myr]
s000001_phot	0.161	4.881×10^8	5.520×10^8					167.441	115.072
s000001_photEW	0.174	4.802×10^8	5.437×10^8					165.732	114.860
s000001_photspec	0.581	4.975×10^8	3.518×10^8					143.278	112.947
s000001_photspecEW	0.581	4.959×10^8	3.516×10^8					142.921	113.134
s000003_phot	0.403	1.253×10^9	6.849×10^8					756.344	203.233
s000003_photEW	4.909	1.103×10^9	5.106×10^8					804.932	191.292
s000003_photspec	0.798	1.019×10^9	4.441×10^8					780.895	201.972
s000003_photspecEW	0.932	9.955×10^8	3.611×10^8					870.734	176.764
s000010_phot	0.153	7.078×10^8	6.029×10^8					159.784	111.616
s000010_photEW	0.163	6.568×10^8	5.522×10^8					148.773	109.558
s000010_photspec	0.639	1.820×10^9	6.707×10^8					276.395	81.574
s000010_photspecEW	0.638	1.845×10^9	6.641×10^8					279.228	79.793

Stellar masses and stellar ages are mostly consistent, whatever the dataset

Object	z	$M/M_\odot$
s000001	11.4	$(4.96 \pm 3.52)\ 10^8$
s000003	4.9	$(9.96 \pm 3.61)\ 10^8$
s000010	11.0	$(1.85 \pm 0.66)\ 10^9$

Fitting photometric, spectroscopic and equivalent widths / line fluxes

id	χ^2_ν	M_{star} $[M_\odot]$	M_{star_err} $[M_\odot]$	SFR_{10Myrs} $[M_\odot yr^{-1}]$	SFR_{10Myrs_err} $[M_\odot yr^{-1}]$	A_V $[M_\odot yr^{-1}]$	A_{V_err} $[M_\odot yr^{-1}]$	age_{main} [Myr]	age_{main_err} [Myr]
s000001_phot				27.921	4.483	0.431	0.365	167.441	115.072
s000001_photEW				27.901	4.469	0.429	0.365	165.732	114.860
s000001_photspec				13.423	3.069	0.368	0.174	143.278	112.947
s000001_photspecEW				13.384	3.071	0.366	0.174	142.921	113.134
s000003_phot				26.287	9.905	2.049	0.515	756.344	203.233
s000003_photEW				26.514	11.030	2.099	0.566	804.932	191.292
s000003_photspec				17.100	6.138	1.846	0.393	780.895	201.972
s000003_photspecEW				19.732	7.033	1.915	0.372	870.734	176.764
s000010_phot				36.187	5.235	0.451	0.283	159.784	111.616
s000010_photEW				37.880	5.199	0.455	0.276	148.773	109.558
s000010_photspec				10.497	2.281	0.465	0.147	276.395	81.574
s000010_photspecEW				10.469	2.262	0.463	0.148	279.228	79.793

SFRs and A_V show significant differences when spectroscopy is used

Nebular parameters derived from fitting

id	χ^2_ν	log U	log U_err	n_e	n_e_err	Z_{gas}	Z_{gas_err}	Z_{star}	Z_{star_err}
s000001_phot	0.161	−1.884	0.797	54.573	44.998	0.007	0.005	0.005	0.005
s000001_photEW	0.174	−1.991	0.802	54.773	44.999	0.008	0.005	0.005	0.005
s000001_photspec	0.581	−2.659	0.483	55.447	44.998	0.011	0.004	0.006	0.006
s000001_photspecEW	0.581	−2.685	0.472	55.522	44.997	0.011	0.004	0.006	0.006
s000003_phot	0.403	−2.089	0.195	1000.000	6.915×10^{-13}	0.005	0.003	0.003	0.004
s000003_photEW	4.909	−2.500	3.232×10^{-4}	1000.000	2.274×10^{-13}	0.004	4.992×10^{-5}	2.212×10^{-4}	4.929×10^{-4}
s000003_photspec	0.798	−2.335	0.110	1000.000	1.482×10^{-12}	0.005	9.045×10^{-4}	5.812×10^{-4}	$7.115\times10^{-[illegible]}$
s000003_photspecEW	0.932	−2.500	3.189×10^{-4}	1000.000	9.095×10^{-13}	0.004	3.624×10^{-6}	3.057×10^{-4}	3.821×10^{-4}
s000010_phot	0.153	−1.888	0.795	55.064	45.000	0.006	0.005	0.007	0.005
s000010_photEW	0.163	−2.176	0.447	55.042	45.000	0.008	0.005	0.007	0.005
s000010_photspec	0.639	−2.925	0.278	57.004	44.955	0.007	0.005	0.009	0.005
s000010_photspecEW	0.638	−2.980	0.141	57.132	44.949	0.007	0.005	0.009	0.005

Gas metallicity relatively well constrained

Stellar metallicity not constrained

Fitting photometric, spectroscopic and equivalent widths / line fluxes

id	χ^2_ν	M_{star} [$M_\odot$]	M_{star_err} [$M_\odot$]	SFR_{10Myrs} [$M_\odot yr^{-1}$]	SFR_{10Myrs_err} [$M_\odot yr^{-1}$]	A_V [$M_\odot yr^{-1}$]	A_{V_err} [$M_\odot yr^{-1}$]	age_{main} [Myr]	age_{main_err} [Myr]
s000001_phot	0.161	4.881×10^8	5.520×10^8	27.921	4.483	0.431	0.365	167.441	115.072
s000001_photEW	0.174	4.802×10^8	5.437×10^8	27.901	4.469	0.429	0.365	165.732	114.860
s000001_photspec	0.581	4.975×10^8	3.518×10^8	13.423	3.069	0.368	0.174	143.278	112.947
s000001_photspecEW	0.581	4.959×10^8	3.516×10^8	13.384	3.071	0.366	0.174	142.921	113.134
s000003_phot	0.403	1.253×10^9	6.849×10^8	26.287	9.905	2.049	0.515	756.344	203.233
s000003_photEW	4.909	1.103×10^9	5.106×10^8	26.514	11.030	2.099	0.566	804.932	191.292
s000003_photspec	0.798	1.019×10^9	4.441×10^8	17.100	6.138	1.846	0.393	780.895	201.972
s000003_photspecEW	0.932	9.955×10^8	3.611×10^8	19.732	7.033	1.915	0.372	870.734	176.764
s000010_phot	0.153	7.078×10^8	6.029×10^8	36.187	5.235	0.451	0.283	159.784	111.616
s000010_photEW	0.163	6.568×10^8	5.522×10^8	37.880	5.199	0.455	0.276	148.773	109.558
s000010_photspec	0.639	1.820×10^9	6.707×10^8	10.497	2.281	0.465	0.147	276.395	81.574
s000010_photspecEW	0.638	1.845×10^9	6.641×10^8	10.469	2.262	0.463	0.148	279.228	79.793

Object	z	$M/M_\odot$
s000001	11.4	$(4.96 \pm 3.52)\ 10^8$
s000003	4.9	$(9.96 \pm 3.61)\ 10^8$
s000010	11.0	$(1.85 \pm 0.66)\ 10^9$

MSA-ID-10 galaxy (NIRCam F277W = 27.3 Abmag)

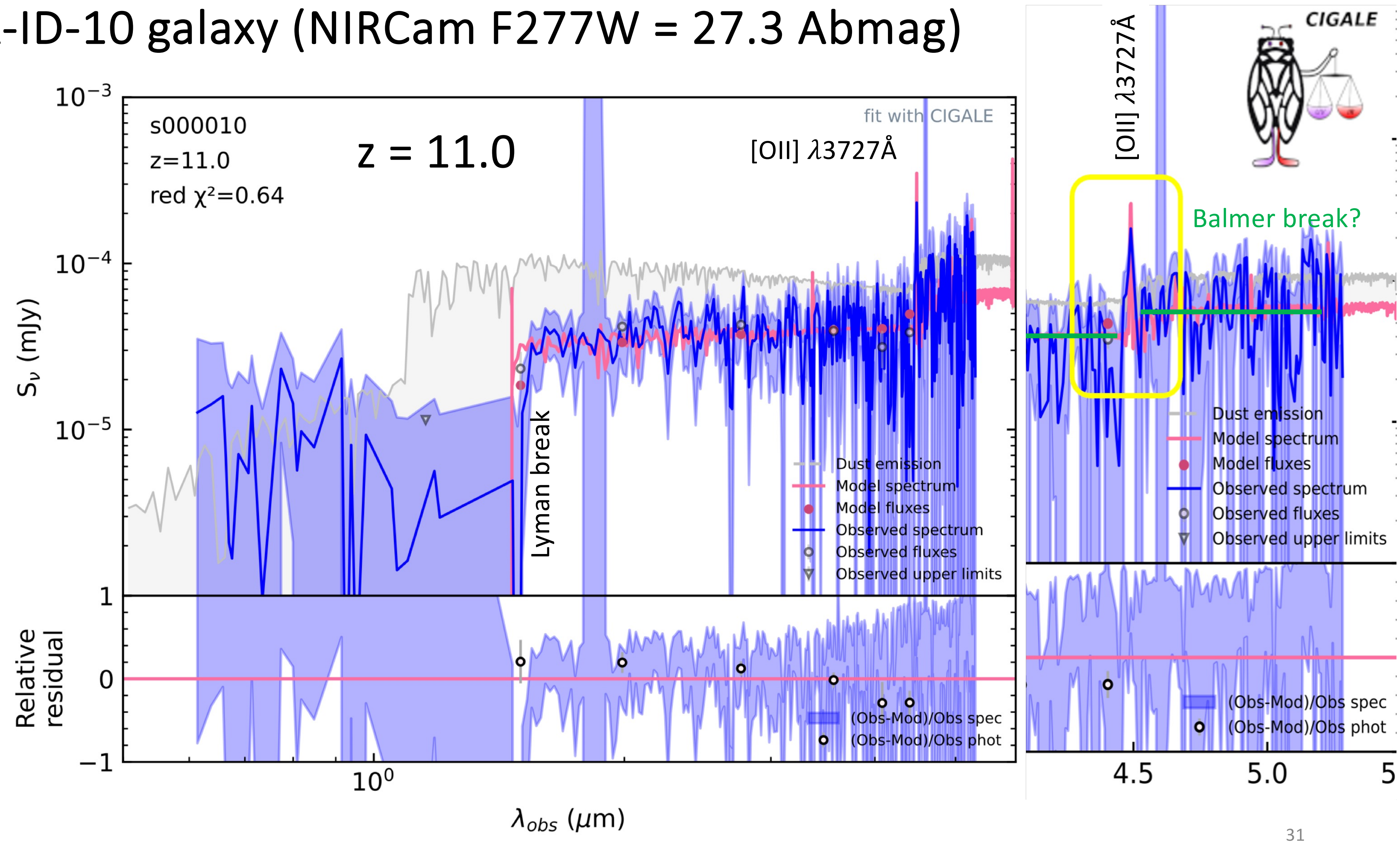

Mass-Metallicity Relation at z ~ 11

Object	z	M/M$_\odot$	Z
s000001	11.4	(4.96 ± 3.52) 10^8	0.011 ± 0.004 (continuum + 1 line)
s000010	11.0	(1.85 ± 0.66) 10^9	0.007 ± 0.005 (continuum + 1 line)

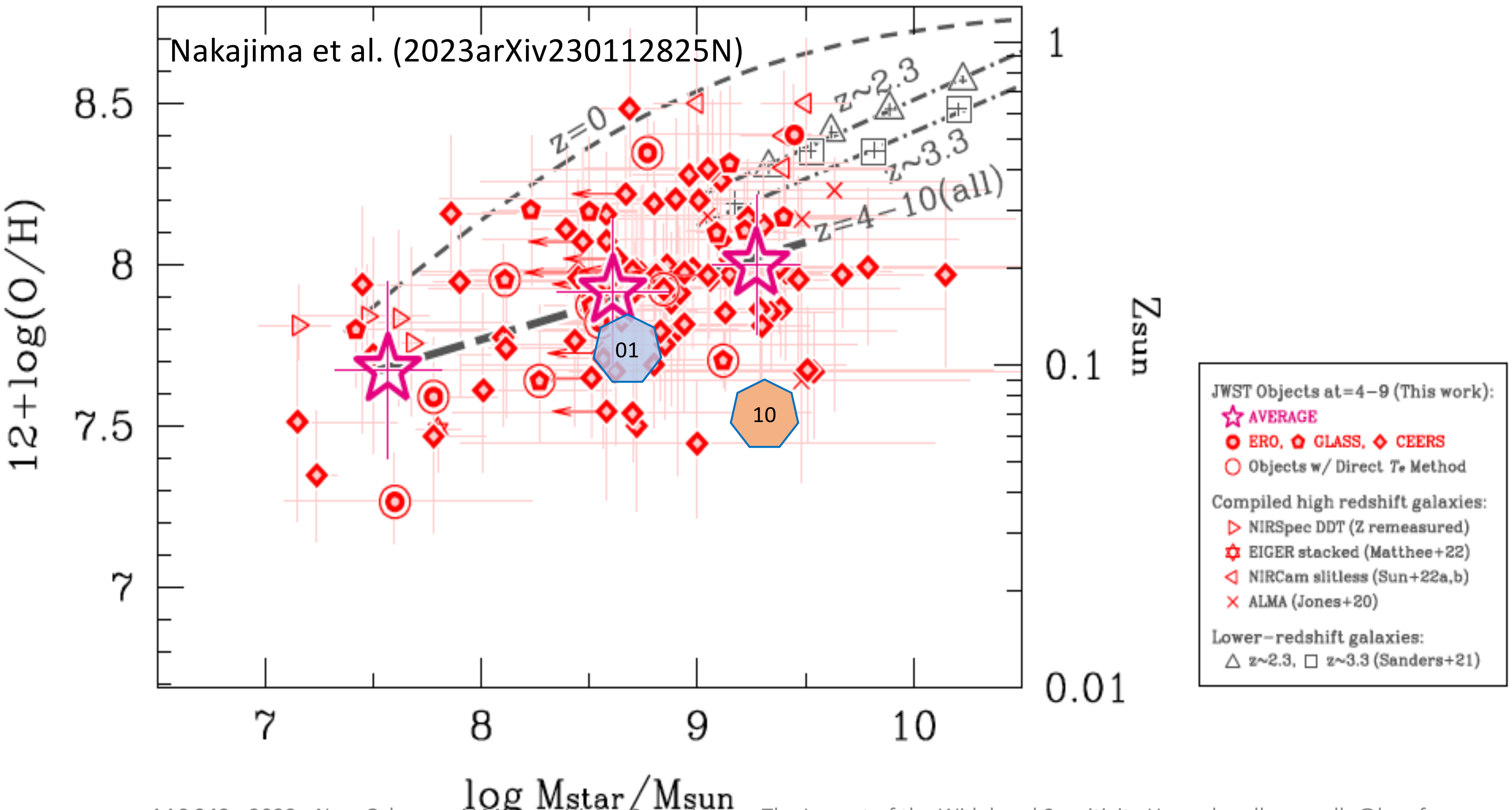

Why the early Universe needs performance in the sub/mm range?

This is related to several hot topics, like:

- The rise of metals and dust in the early Universe
- The first star formation events in the Universe

More specifically, we want:

Objective 1: to **detect the continuum emission** of galaxies to characterize the dust grains, and first of all the dust mass M_{dust}

Objective 2: to **detect the rest-frame far-IR fine-structure lines** to characterize the interstellar medium and confirm redshifts

Objective 3: **not to make mistakes** and correctly identify contaminants / interlopers in high redshift candidate samples

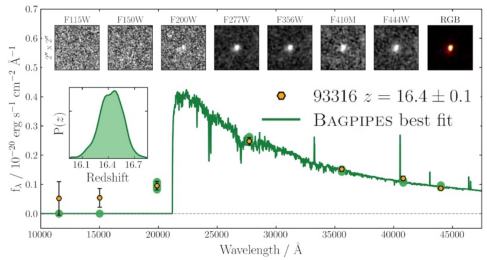

Why the early Universe needs performance in the sub/mm range?

This is related to several hot topics, like:

- The rise of metals and dust in the early Universe
- The first star formation events in the Universe

More specifically, we want:

Objective 1: to **detect the continuum emission** of galaxies to characterize the dust grains, and first of all the dust mass M_{dust}

Objective 2: to **detect the rest-frame far-IR fine-structure lines** to characterize the interstellar medium and confirm redshifts

Objective 3: not to make mistakes and correctly identify contaminants / interlopers in high redshift candidate samples

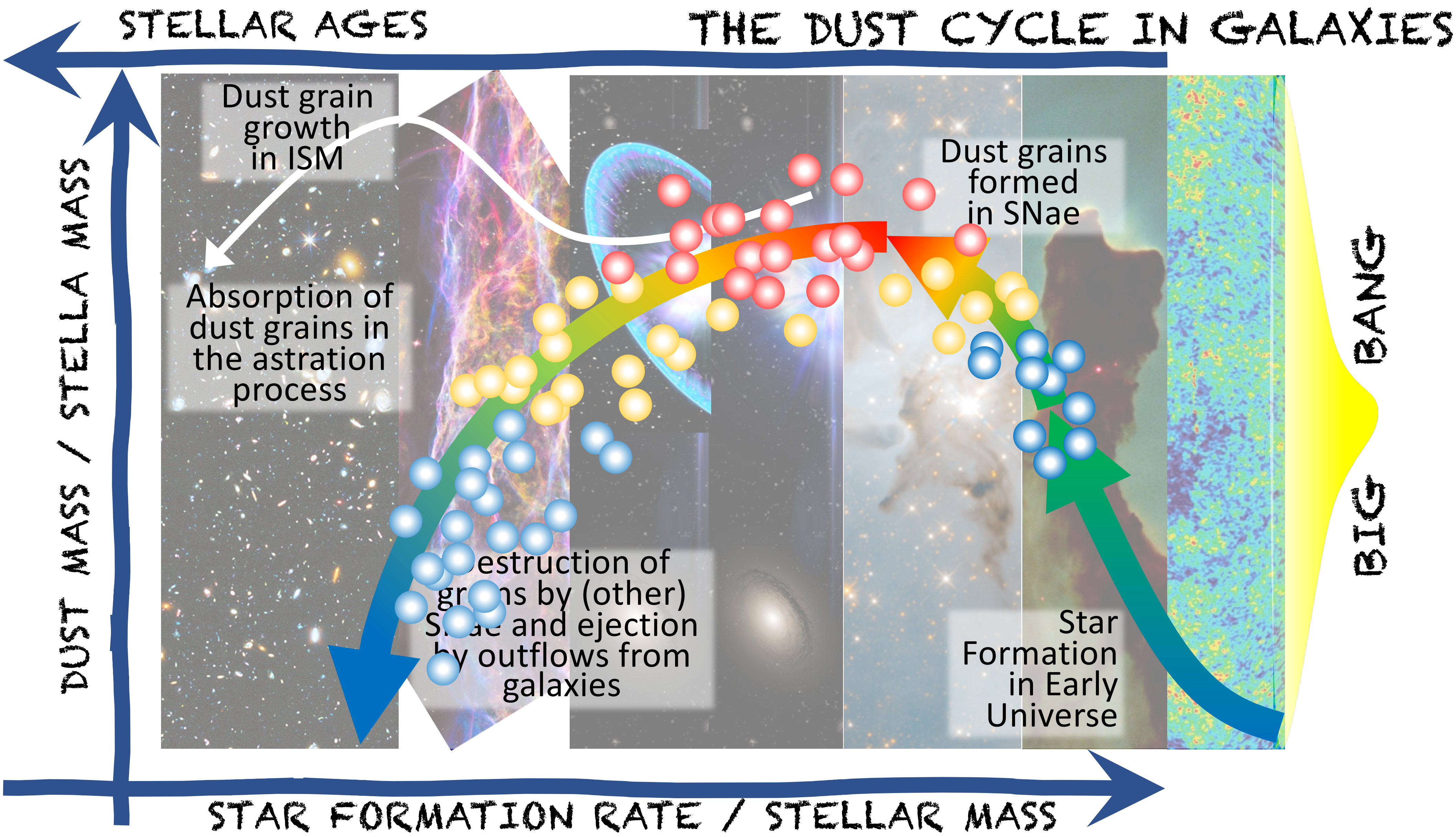

STELLAR AGES
THE DUST CYCLE IN GALAXIES
DUST MASS / STELLA MASS
Dust grain growth in ISM
Absorption of dust grains in the astration process
Dust grains formed in SNae
estruction of gr ns by (other) S ae and ejection y outflows from galaxies
Star Formation in Early Universe
BIG BANG
STAR FORMATION RATE / STELLAR MASS

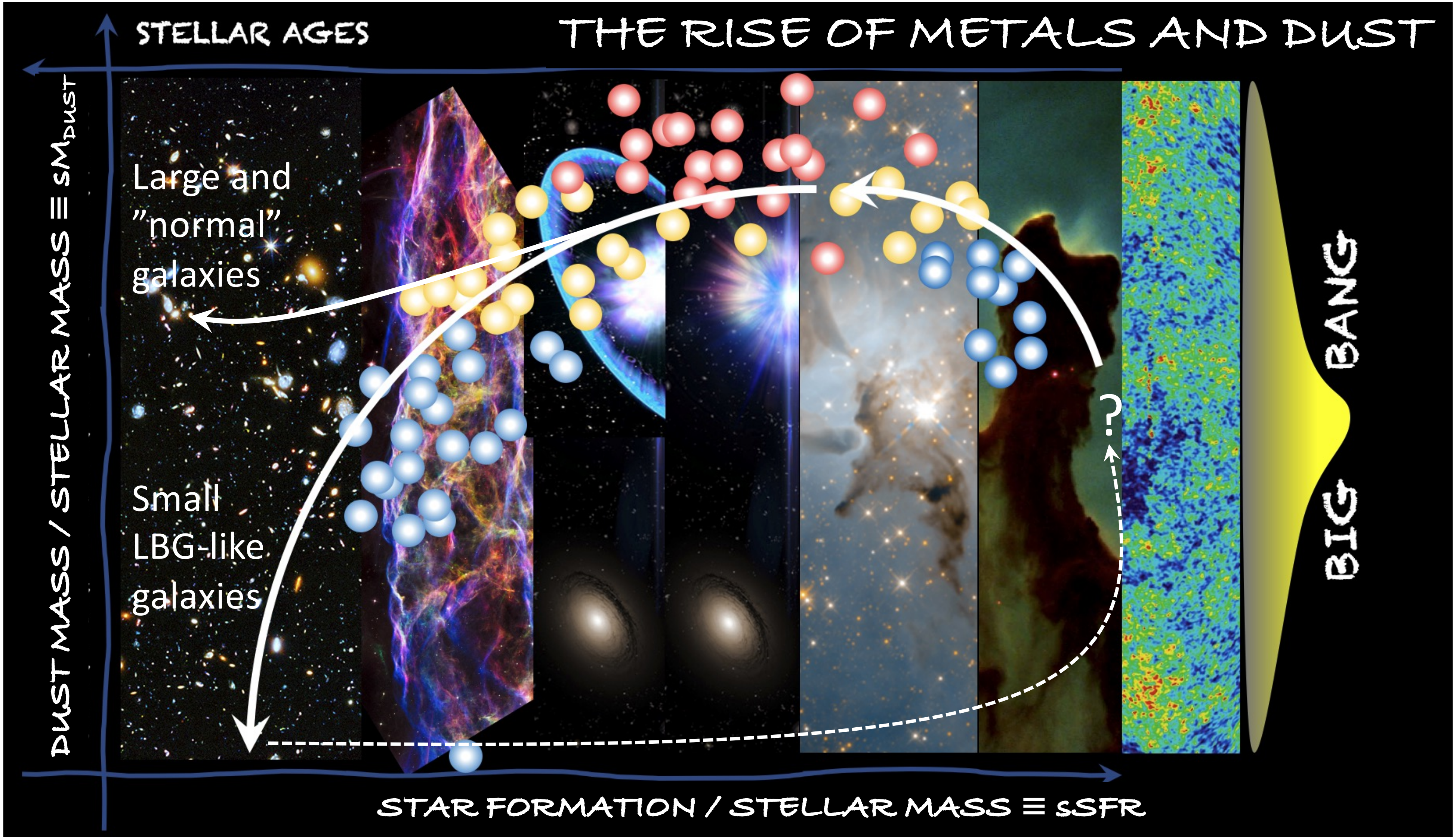
STELLAR AGES
THE RISE OF METALS AND DUST
DUST MASS / STELLAR MASS ≡ sM$_{DUST}$
Large and
"normal"
galaxies
Small
LBG-like
galaxies
?
BIG BANG
STAR FORMATION / STELLAR MASS ≡ sSFR

How to estimate M_{DUST}

The IR SED

$$S_\nu \propto \nu^{\beta_{RJ}} B_\nu(T_{dust})$$

was computed with a modified blackbody

$$B_\nu(T_{dust}) = \frac{2h}{c^2}\frac{\nu^3}{e^{\frac{h\nu}{kT_{dust}}} - 1}$$

and the dust mass was derived with the following formula:

$$M_{dust} = \frac{L_\nu}{4\pi\kappa_\nu B_\nu\boxed{(T_{dust})}}$$

Derived from the fit

K_ν is the dust mass absorption coefficient

Model-dependant

$$\kappa_\nu = \boxed{\kappa_0}(\nu/\nu_0)^{\boxed{\beta_{RJ}}}$$

where ν_0 is the frequency where the optical depth equals unity and β_{RJ} is the spectral emissivity index from the Rayleigh-Jeans range.

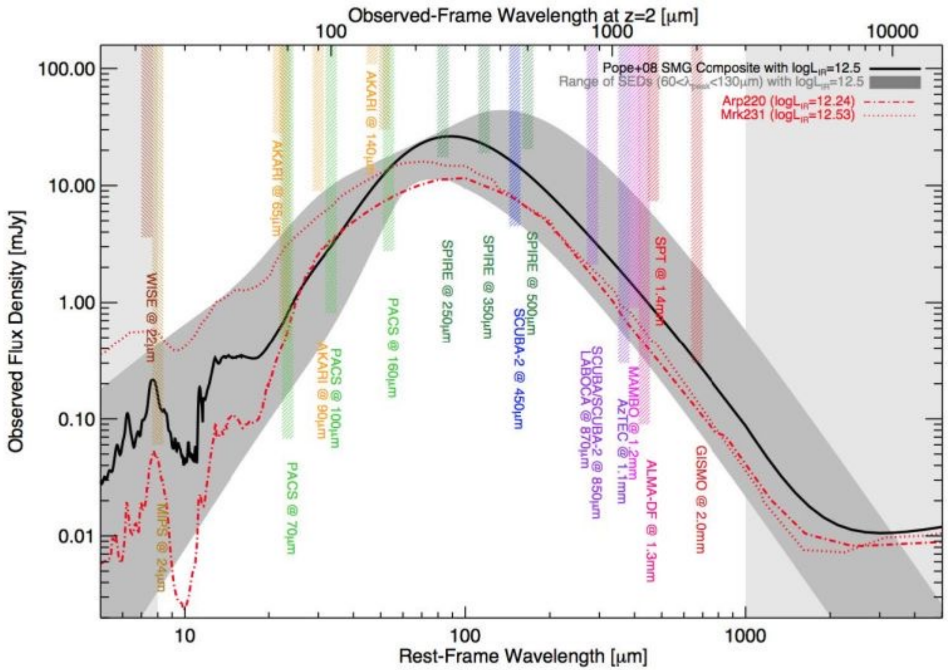

https://ned.ipac.caltech.edu/level5/Sept15/Casey/Casey2.html

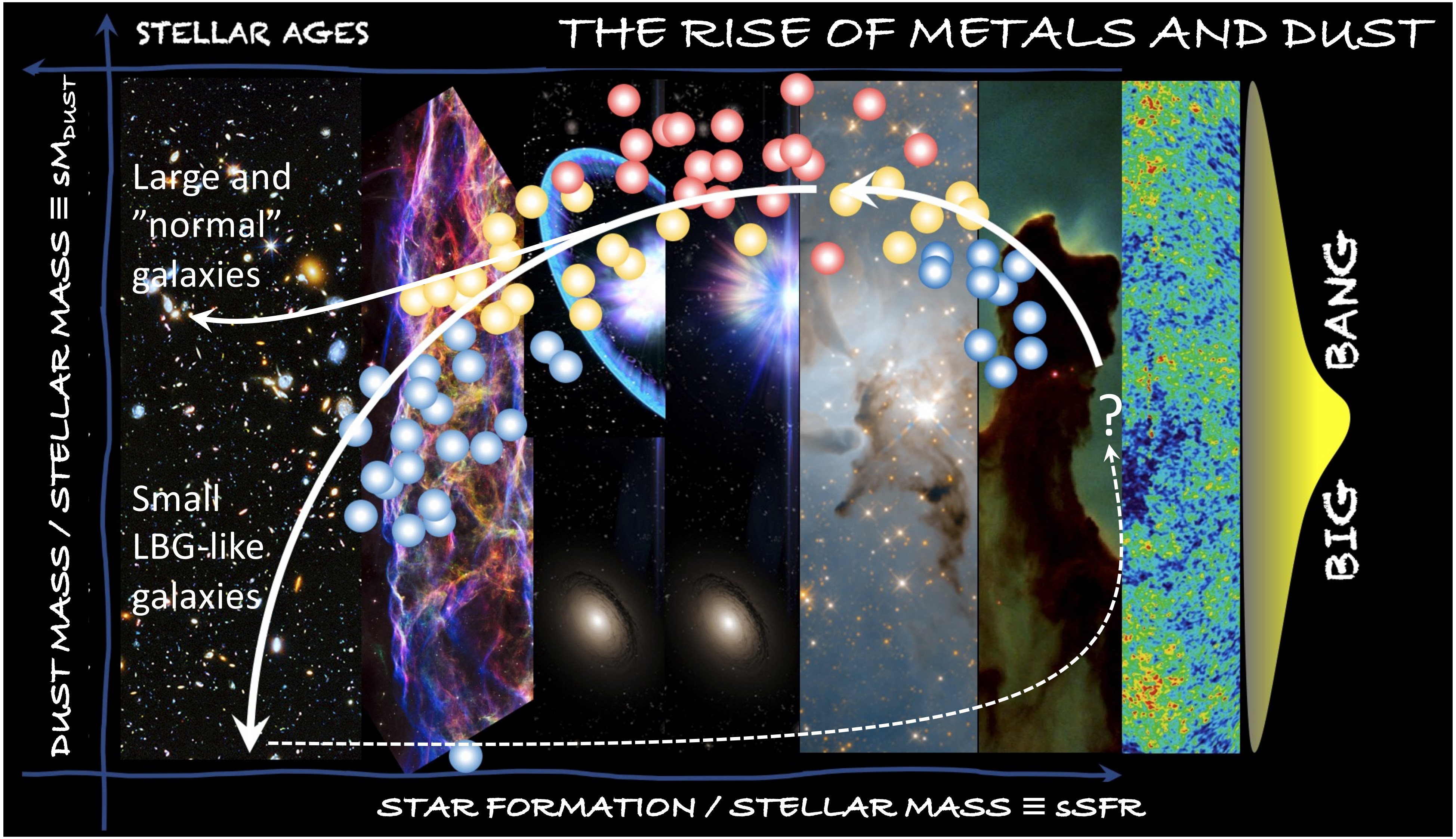

STELLAR AGES
THE RISE OF METALS AND DUST
DUST MASS / STELLAR MASS ≡ sM$_{DUST}$
Large and
"normal"
galaxies
Small
LBG-like
galaxies
?
BIG BANG
STAR FORMATION / STELLAR MASS ≡ sSFR

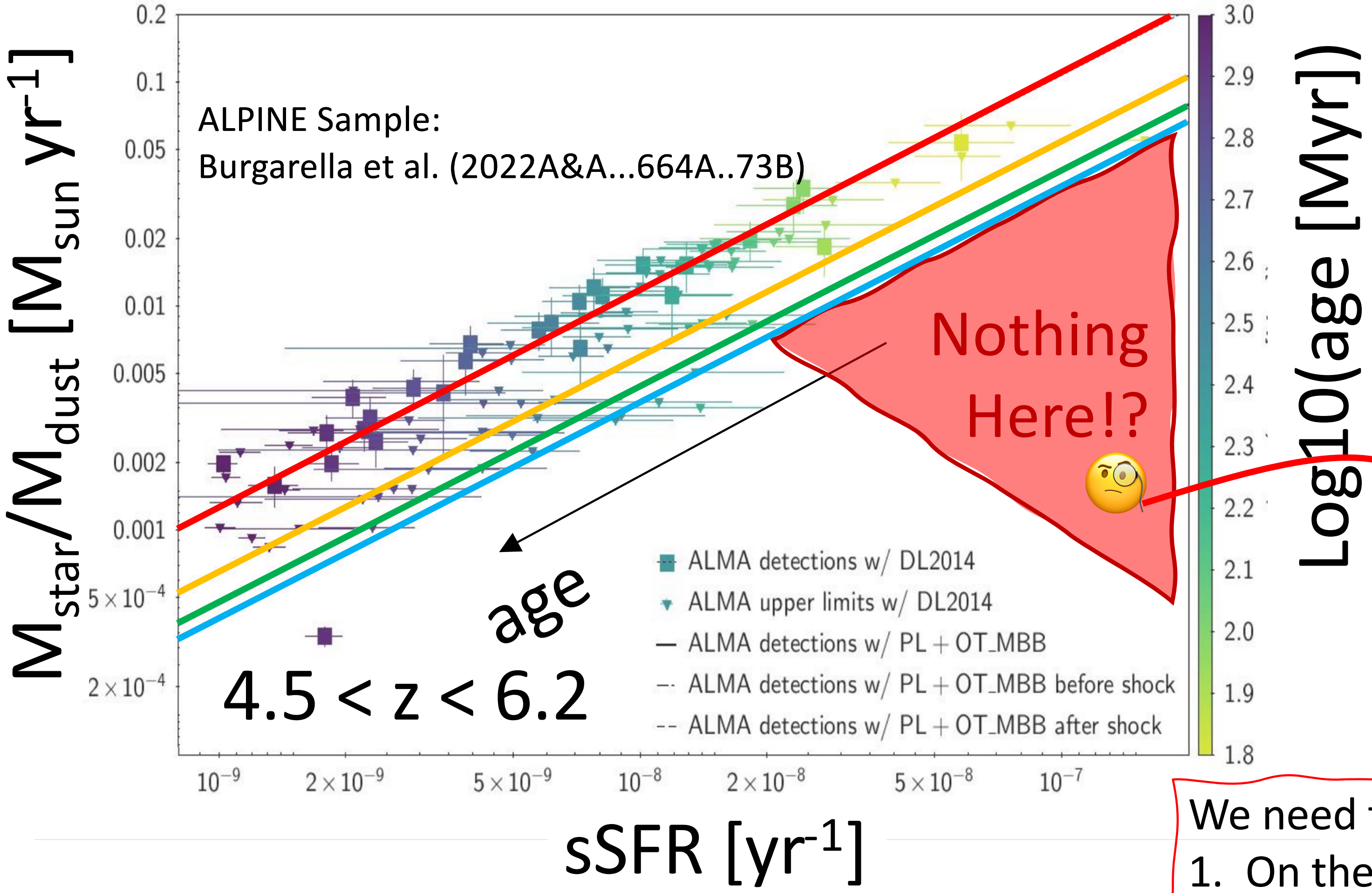

We need to push:

1. On the x-axis to higher sSFR objects
2. On the y-axis to lower M_{star}/M_{dust} objects

39

Why the early Universe needs performance in the sub/mm range?

This is related to several hot topics, like:

- The rise of metals and dust in the early Universe
- The first star formation events in the Universe

More specifically, we want:

Objective 1: to **detect the continuum emission** of galaxies to characterize the dust grains, and first of all the dust mass M_{dust}

Objective 2: to **detect the rest-frame far-IR fine-structure lines** to characterize the interstellar medium and confirm redshifts

Objective 3: **not to make mistakes** and correctly identify contaminants / interlopers in high redshift candidate samples

Redshifts

For instance, in Fujimoto, Finkelstein, Burgarella et al. (2023ApJ...955..130F): “two of the most unique, highest-z candidates are CEERS-93316 (Donnan et al. 2023) and S5-z17-1 (Harikane et al. 2023). These candidates exhibit a clear “dropout” color signature and blue continuum slopes in NIRCam filters, interpreted as the redshifted Lyα break at z~17.“

The Astrophysical Journal, 955:130 (21pp), 2023 October 1

Fujimoto et al.

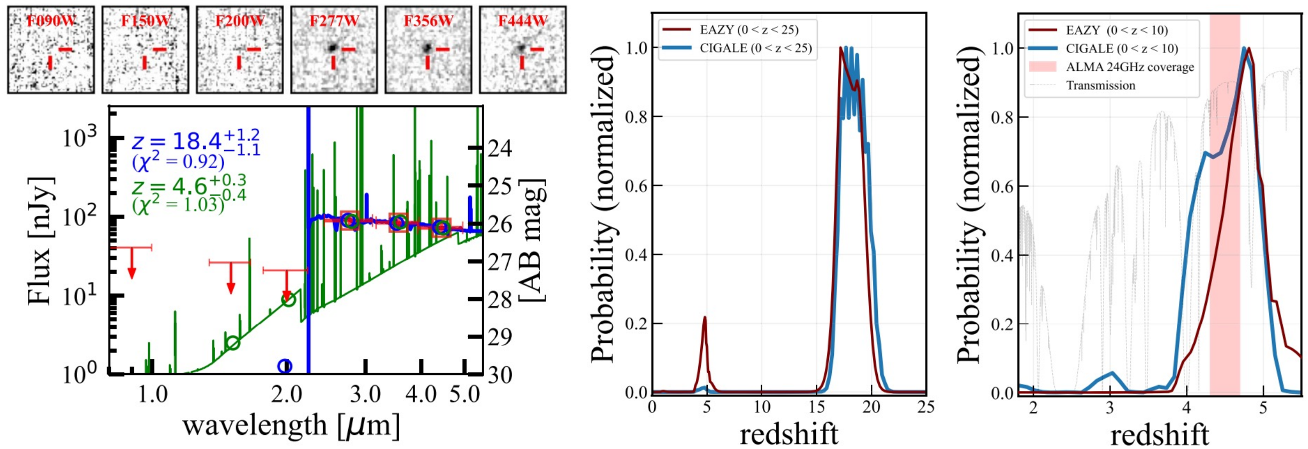

Figure 1. Left: the NIR SED of S5-z17-1. The red circles and arrows indicate the observed flux densities and 2σ upper limits, respectively. The blue and green curves and redshift labels represent the best-fit model SEDs and photometric redshifts by CIGALE with the redshift range at $0 < z < 25$ and $0 < z < 10$, respectively. The blue and green open circles are predicted flux densities in the NIRCam filters based on the best-fit SEDs. The low-z forced SED has a brighter submillimeter flux by >100 times than the best-fit high-z SED, expecting a $\sim 10\sigma$ detection from the ALMA Band 7 observation (gray curve in Figure 3). The images on this panel present $2'' \times 2''$ NIRCam cutout images of S5-z17-1. Middle: $P(z)$ from the SED fitting by EAZY (brown curve) and CIGALE (light blue curve) with a redshift range at $0 < z < 25$. Right: same as the middle panel, but at $0 < z < 10$. The gray dashed line denotes the atmospheric transmission for [C II]. The red shade indicates the [C II] redshift range of $z = 4.31$–4.69 covered by our ALMA Band 7 observations spanning 334–358 GHz with three frequency tunings, which is optimized to maximally cover the peak of the lower-redshift solution's $P(z)$ and avoid the significantly low atmospheric transmission.

Redshifts

For instance, in Fujimoto, Finkelstein, Burgarella et al. (2023ApJ...955..130F):
"the natural and tapered maps achieved an FWHM size of the synthesized beam of 0.77''×0.46'' with 1σ sensitivities for the continuum of 45.0 μJy and the line in a 60 km s−1 width channel of 770 μJy beam^{-1}."

THE ASTROPHYSICAL JOURNAL, 955:130 (21pp), 2023 October 1 Fujimoto et al.

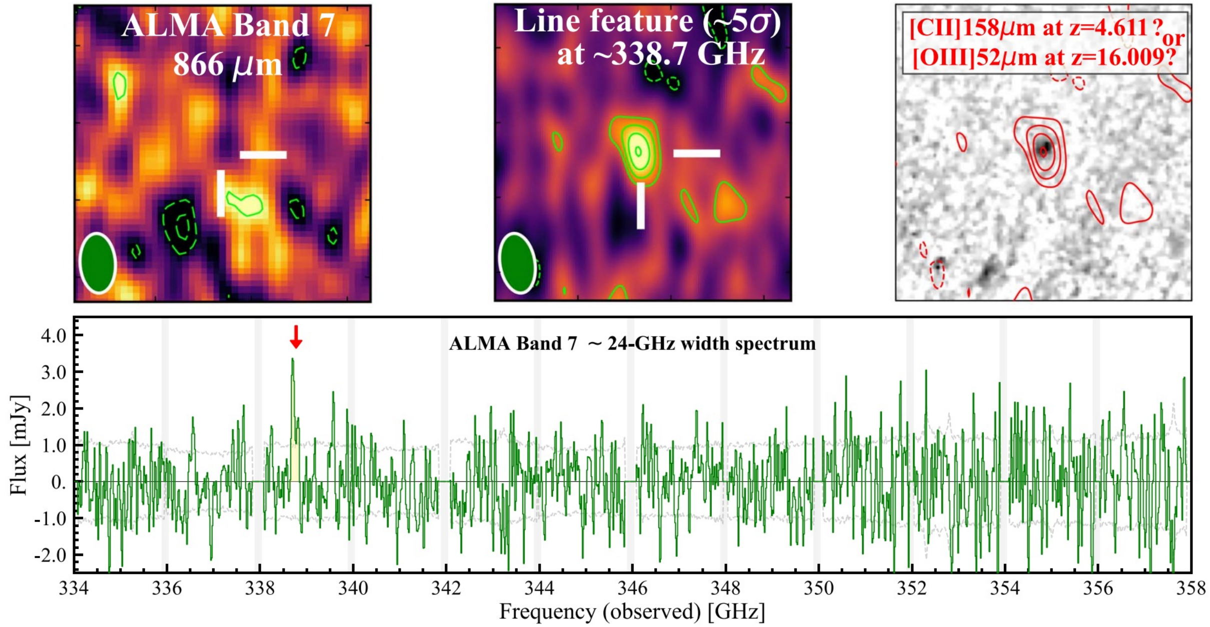

Figure 2. ALMA Band 7 observation results. Top: ALMA 4″ × 4″ × cutout of the continuum at 866 μm (left), the velocity-integrated map for the 5.1σ line feature at around 338.7 GHz (middle), JWST/NIRCam F356W image (right). The dashed contours indicate the −2σ and −3σ levels, while the solid contours denote the 2σ, 3σ, 4σ, and 5σ levels. The red contours overlaid on the F356W image indicate the line intensity in the moment-0 map. The green ellipse shows the ALMA synthesized beam. Bottom: ALMA ∼24 GHz width spectrum (green) obtained from three frequency setups. The gray dashed line denotes the 1σ noise per channel. The gray shades show 120 MHz gaps between basedbands.

THE ASTROPHYSICAL JOURNAL, 955:130 (21pp), 2023 October 1 Fujimoto et al.

Table 1
ALMA DDT Observation and Data Properties for S5-z17-1

Freq. Setup	Baseline (m)	N_{ant}	Frequency (GHz)	T_{int} (minutes)	PWV (mm)	Beam ($'' \times ''$)	$\langle\sigma_{line}\rangle$[a] ($\mu$Jy beam^{-1})	σ_{cont}[a] (μJy beam^{-1})
Tuning1	15.1–629.3	43	334.02–337.90, 346.02–349.96	5.65	0.4	0.77 × 0.46	741	78.8
Tuning2	15.1–629.3	42	338.02–341.90, 350.02–352.96	5.65	0.5	0.77 × 0.46	810	86.1
Tuning3	15.1–629.3	42	342.02–345.90, 354.02–357.96	5.65	0.4	0.77 × 0.46	759	80.7
Combined	⋯	⋯	∼334–358	16.95	⋯	0.77 × 0.46	770	45.0

Why the early Universe needs performance in the sub/mm range?

This is related to several hot topics, like:

- The rise of metals and dust in the early Universe
- The first star formation events in the Universe

More specifically, we want:

Objective 1: to **detect the continuum emission** of galaxies to characterize the dust grains, and first of all the dust mass M_{dust}

Objective 2: to **detect the rest-frame far-IR fine-structure lines** to characterize the interstellar medium and confirm redshifts

Objective 3: not to make mistakes and correctly identify contaminants / interlopers in high redshift candidate samples

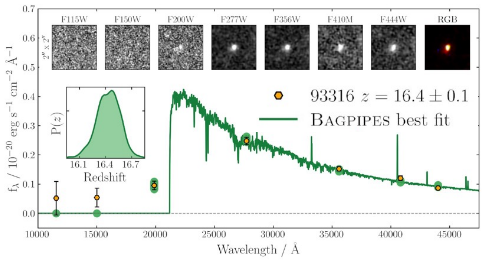

DSFG-1: a dusty starburst masquerading as an ultra-high redshift galaxy in JWST CEERS observations (Zavala et al. 2023)

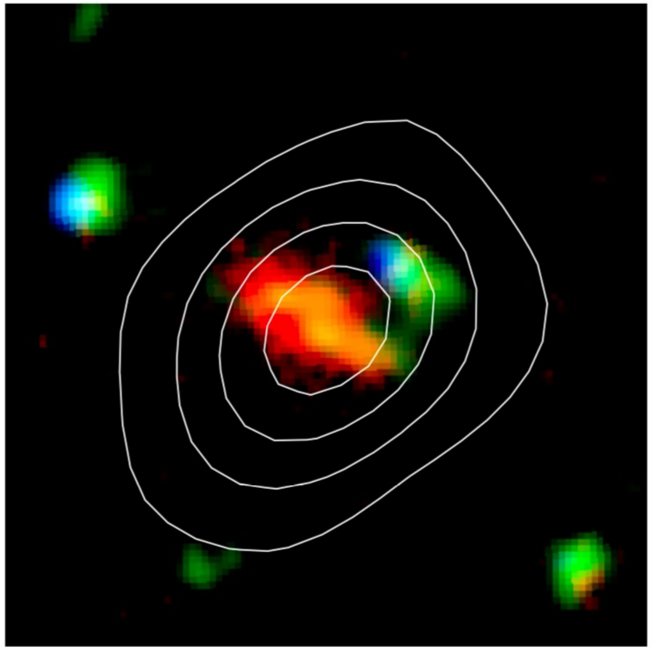

Figure 1. A 3.″0 × 3.″0 composite image centered at the position of CEERS-DSFG-1; the JWST/NIRCam F115W observations are in blue, F277W in green, and F444W in red (the data has been smoothed to roughly match the F444W resolution for better visualization). The 1.1 mm NOEMA signal-to-noise ratio levels starting at 2.5σ to 10σ (in steps of 2.5σ) are represented by the white contours, clearly indicating that the dust thermal emission detected at submillimeter/millimeter wavelengths corresponds to the position of CEERS-DSFG-1.

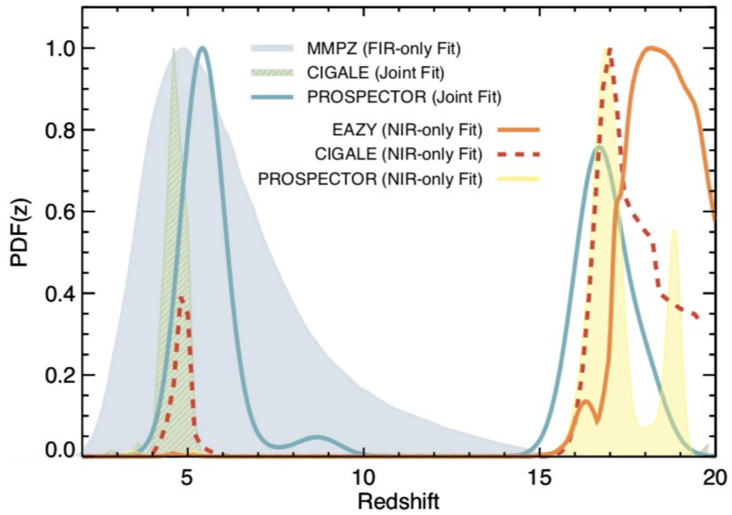

Figure 4. Normalized redshift probability density distributions for CEERS-DSFG-1 from all of the different SED fitting and photometric redshift fitting techniques used. The broadest and less certain fit is from the (sub-)mm wavelength constraints only using MMPz (Casey 2020), favoring $z \sim 5$ (solid light blue distribution). Fits using only JWST photometry in the near-infrared include EAZY (Brammer et al. 2008) with $z \sim 18$, CIGALE (Boquien et al. 2019) with $z \sim 17$, and Prospector with $z \sim 17$. Note that the CIGALE fit results in a bimodal distribution with a secondary peak at $z \sim 5$, but the favored solutions are those at higher redshifts. On the other hand, the CIGALE and Prospector fits that use both (sub)millimeter constraints in addition to JWST photometry favor a $z \sim 5$ solution in both cases (although the Prospector fit still shows a secondary peak at $z \sim 17$).

On-going NOEMA program in CEERS field

Credit: Jorge Zavala

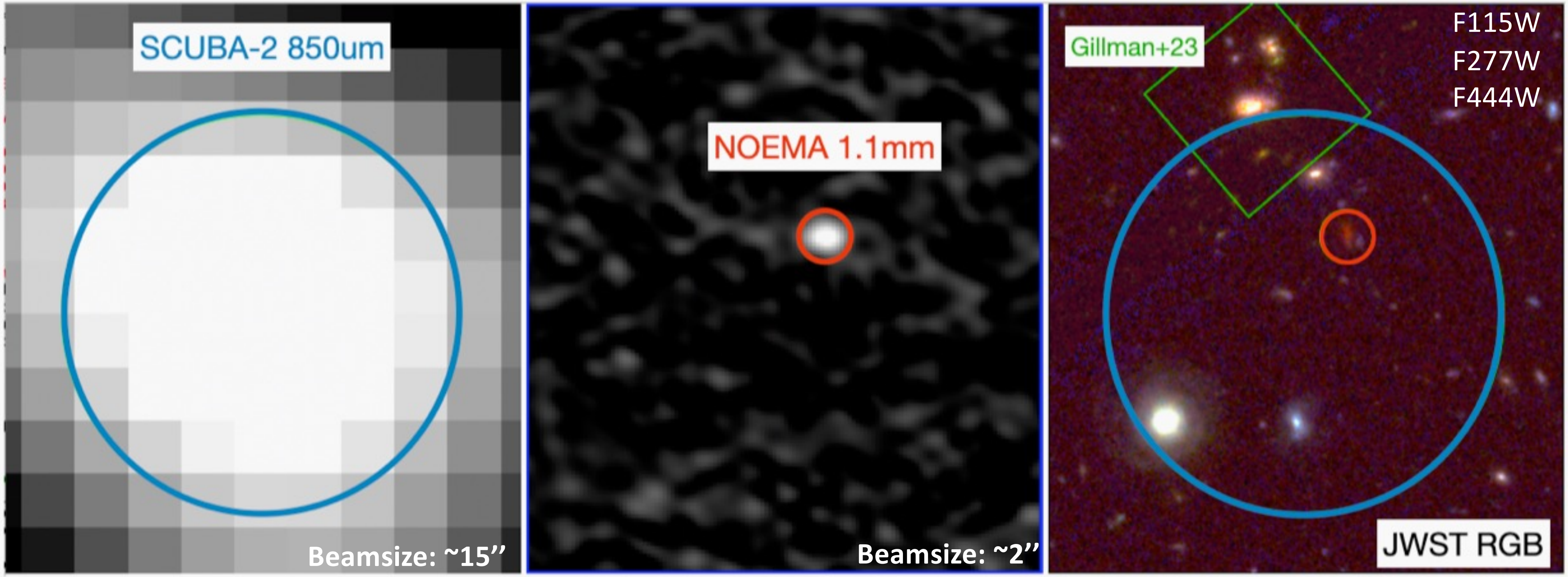

The counterpart that Gillman+23 associated to **DSFG-1**, (based on colors and predicted millimeter fluxes for all the galaxies in the field) missed the good counterpart.
Besides, including (sub-)mm fluxes in the SED fittings is crucial to derive the properties of this kind of galaxies (remember Romain Meyer’s talk on Wednesday).

DSFG-1: photo-z determination

- NIRcam-only (no SCUBA2 & NOEMA) very uncertain, predominence of low-z (3 < z < 5) & a weak probability at high z (z ~ 13)
- Joint-fit (full dataset) gives a narrow PDF-z at z = 5.1 (+/-0.6)

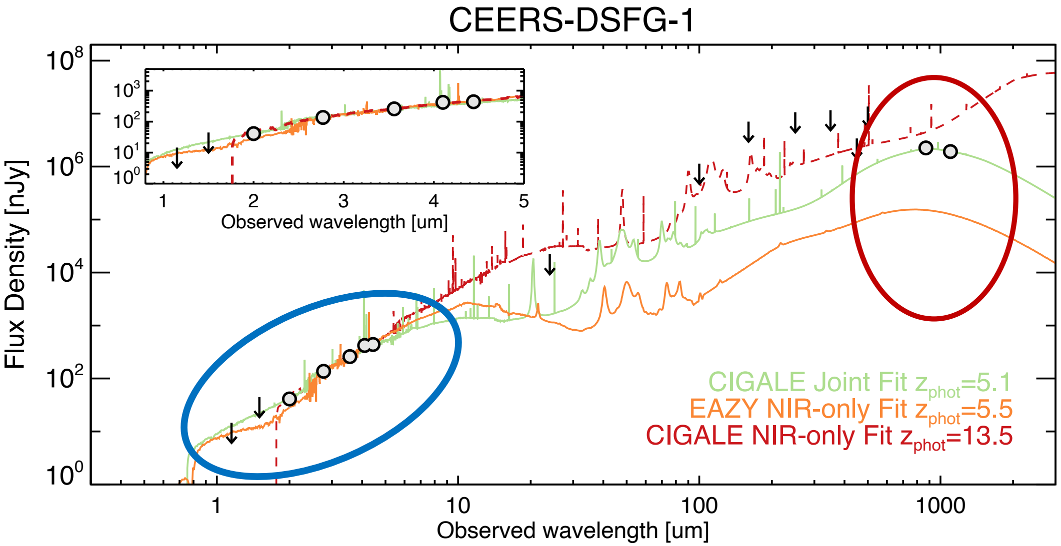

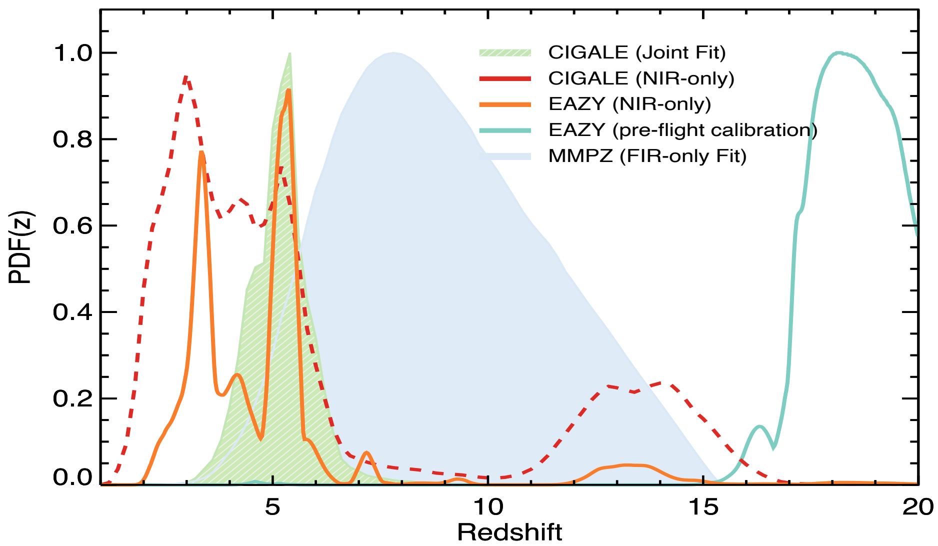

DSFG-1 (NIRCam F277W = 26.2 ABmag)

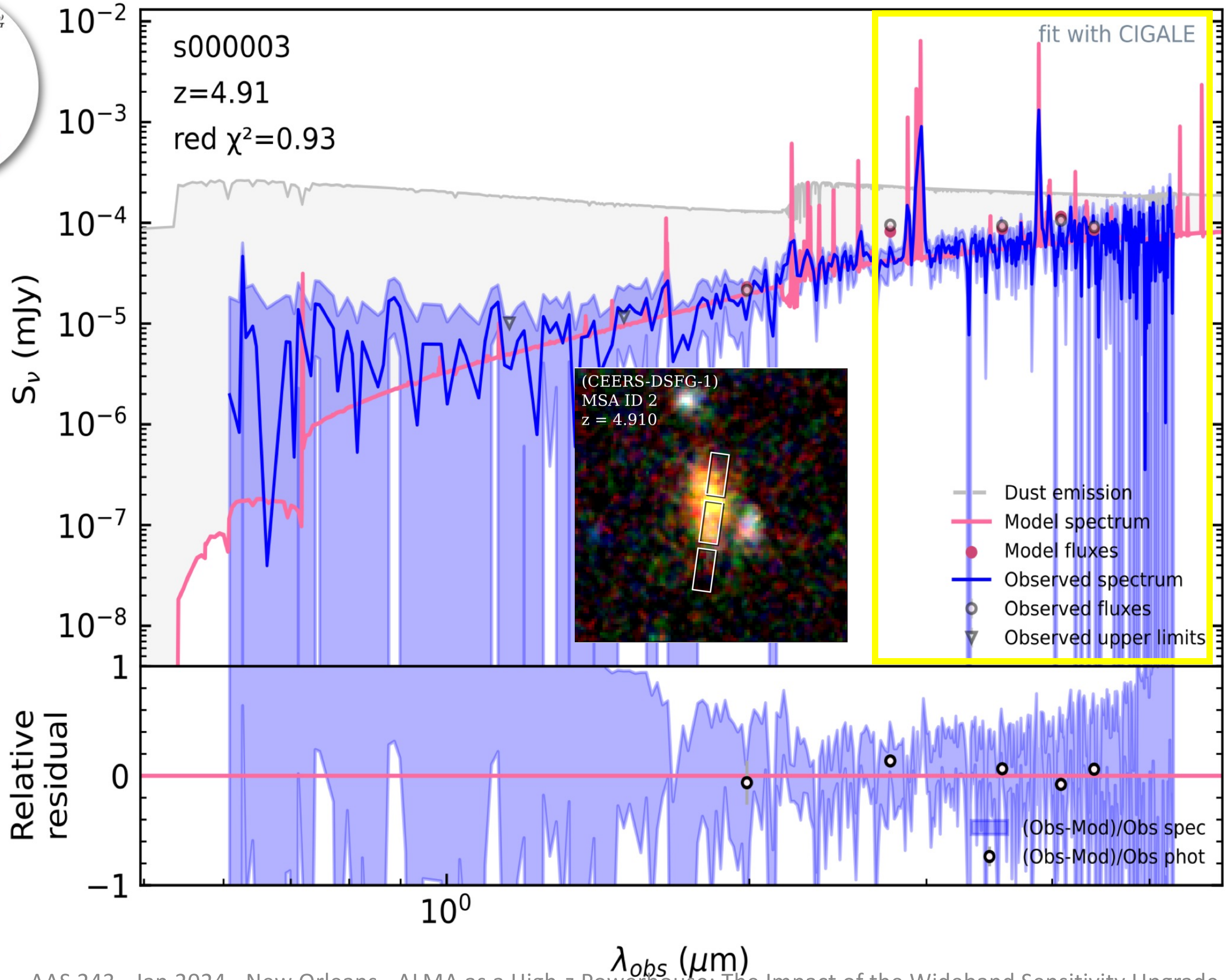

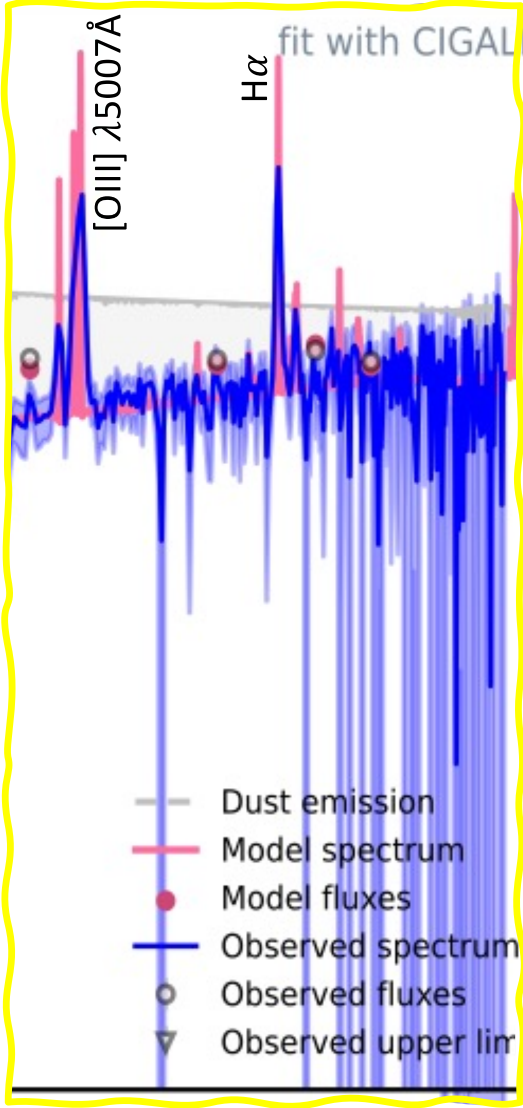

Meyer et al. (2023) identified several similar objects

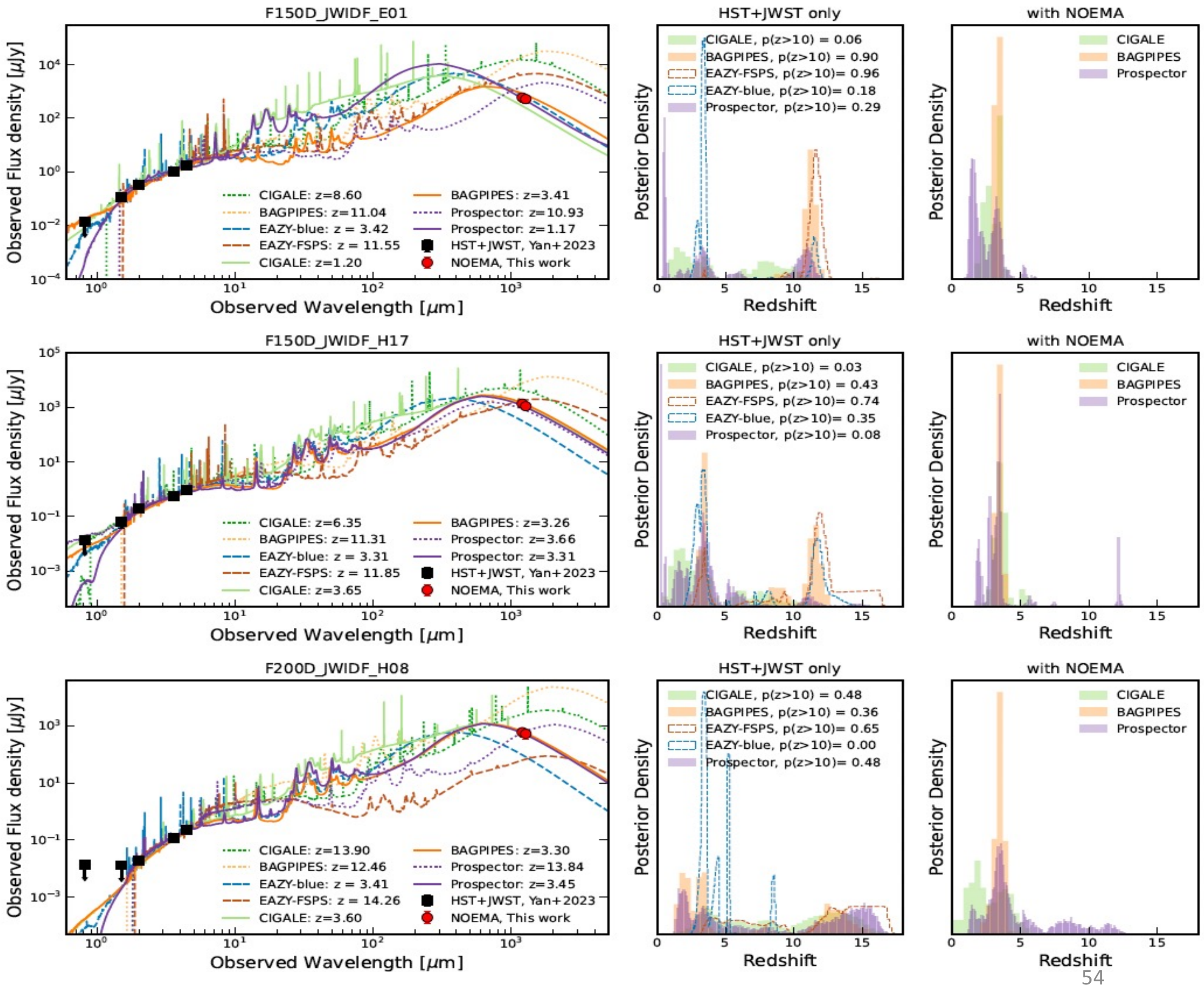

CEERS-93316

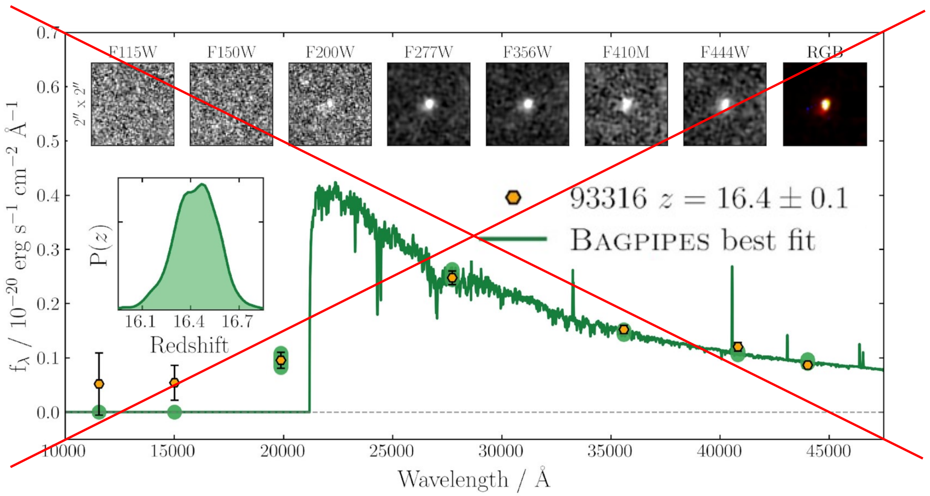

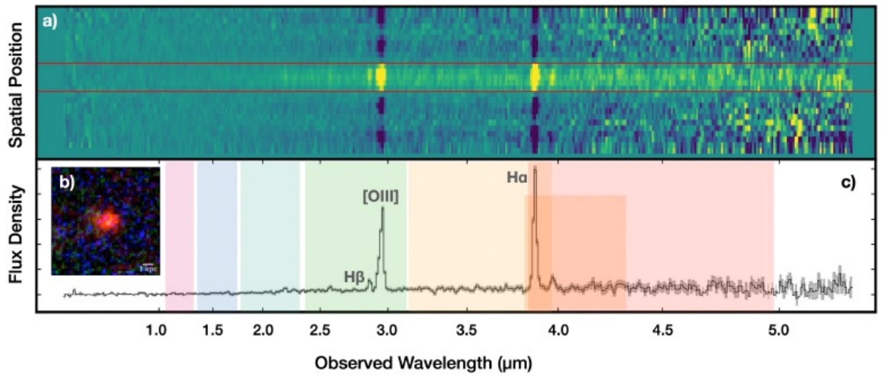

z ~ 16 (Donnan+23)

A less probable z~5 redshift: either a quiescent galaxy or a dusty star forming galaxy with strong emission lines.

Not detected with NOEMA

z ~ 5 overdensity in the field
(Naidu et al. 23, Zavala+ et al. 23)

DSFG-1 and CEERS 93316 are main-sequence galaxies at z ~ 5

From CIGALE's fit

EW	Hβ	OIII 496	OIII 500.8	Hα
Data	9.1 [2.8]	23.7 [8.1]	70 [29]	63.5 [26.9]
bayes	10.3 [1.9]	21.2 [4.3]	65.9 [13.2]	60.9[11.3]

A_V=1.8 [0.4] mag

logU=-1.3 [0.5]

Z_{gas}= 0.003 [0.002]

SFR=13 [5] $M_{sun}\ yr^{-1}$

M_{star} = 16 [6] $10^8\ M_{sun}$

L_{IR}= $10^{11}\ L_{sun}$

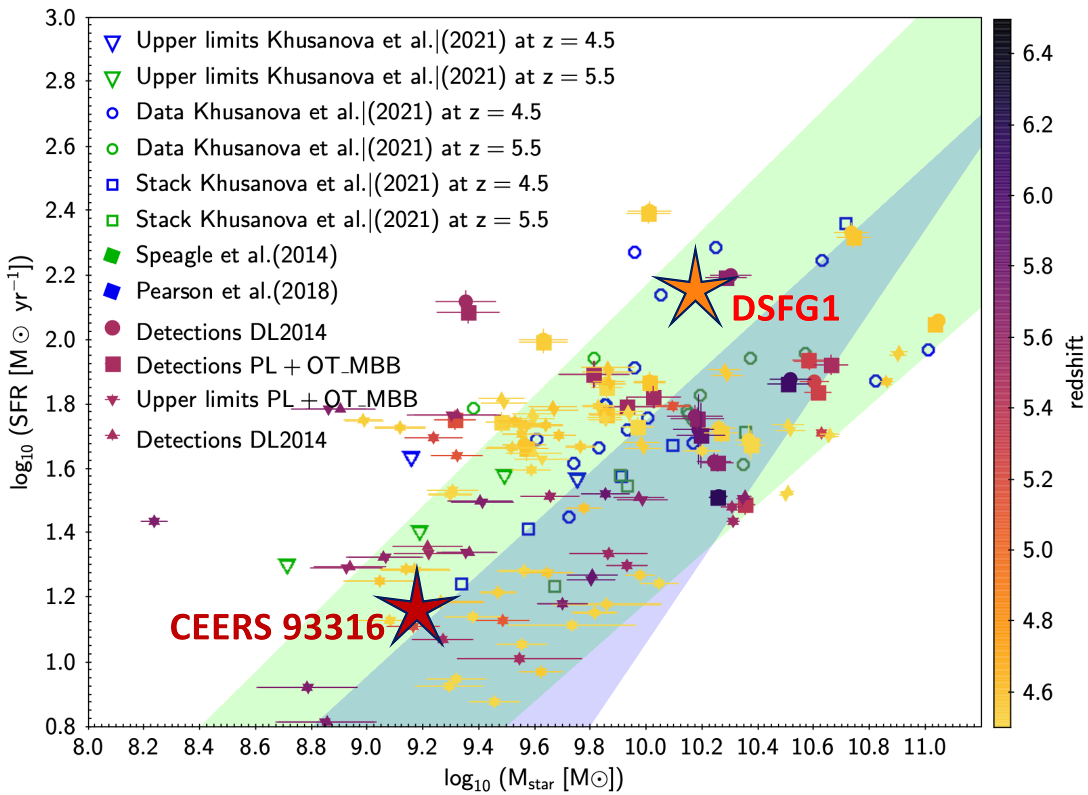

SED fitting of the full dataset (NIRCam photometry and NIRspec EW)

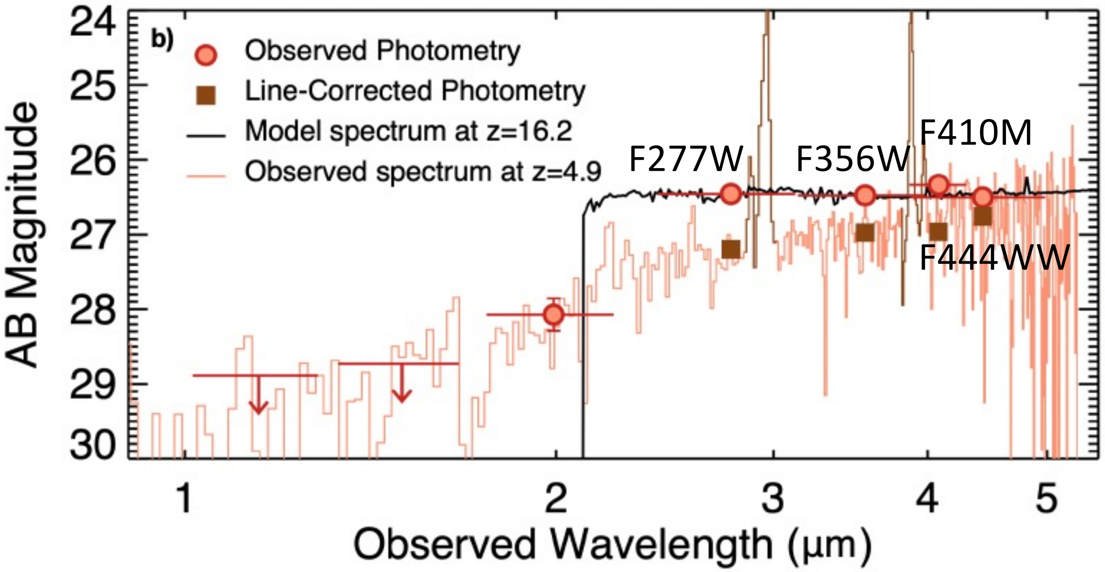

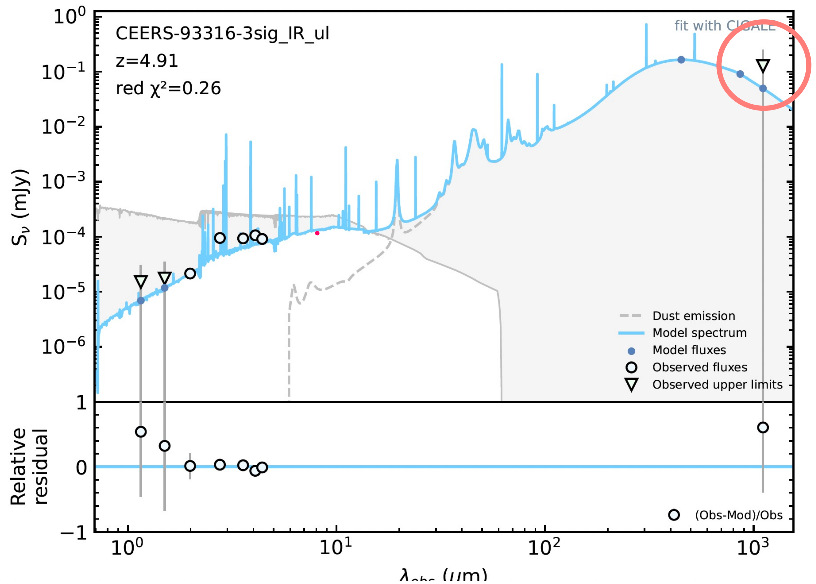

See also McKinney+23, Perez-Gonzalez+22, Naidu+22

CEERS

SED fitting of the full dataset (NIRCam photometry and NIRspec EW)

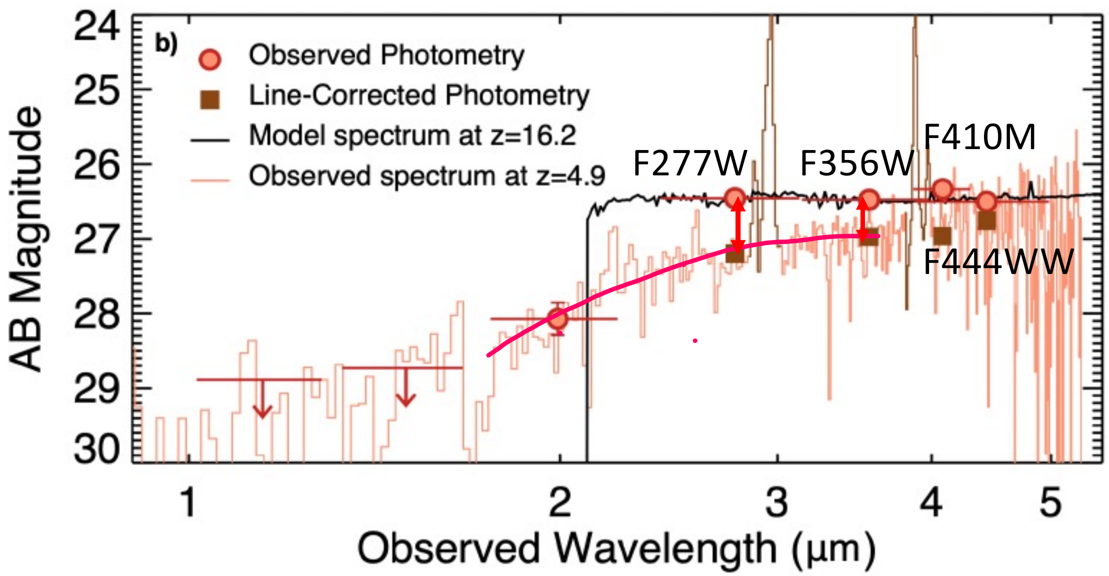

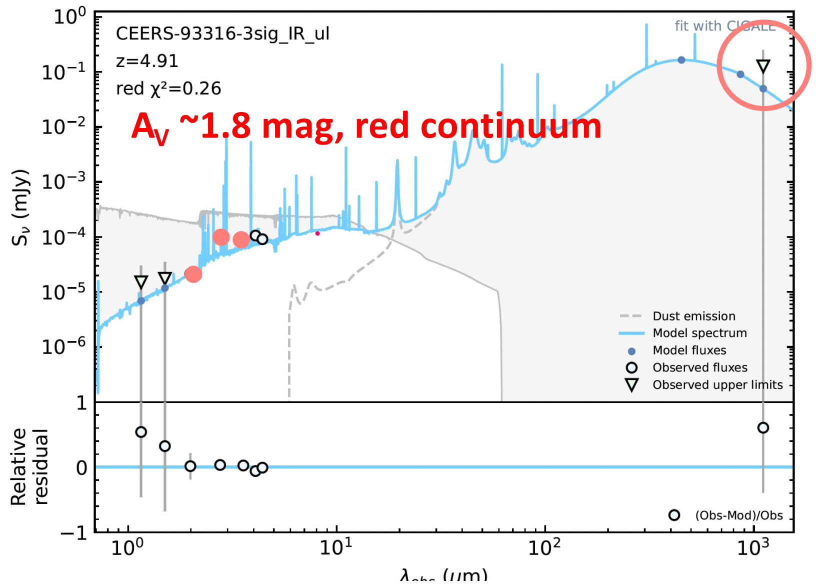

z~4-5 dusty sources with strong emission lines confirmed
as intruders in the quest of ultra hi-z galaxies

See also McKinney+23, Perez-Gonzalez+22, Naidu+22

The End

Thank You

Merci

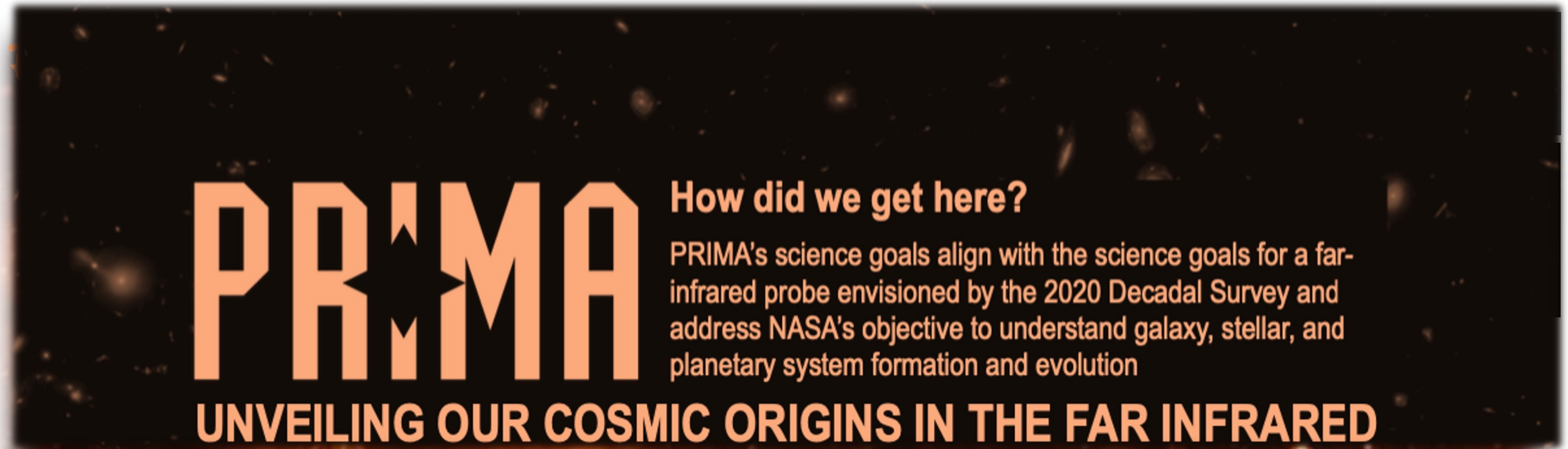

- PRIMA is a cryogenic space telescope project.
- PRIMA is developed by an international team led by JPL and GSFC.
- LAM is presently leading the PRIMAger effort.

https://prima.ipac.caltech.edu

PRIMA is a 1.8m telescope, cooled to 4.5K, placed in L2 orbit. PRIMA is composed of two instruments.

- **FIRESS** (Far-InfraRed Enhanced Survey Spectrometer) **carried by JPL** and will be a medium (R=130) and high (R=2000) resolution spectrometer observing the wavelength range from 25 to 235 um. French laboratories are not involved in this instrument.
- The principle of the NASA call integrating the possibility of non-US contributions, CNES negotiated with JPL a **major role for France** via the supply of a "PRIMAger" IR camera. **PRIMAger** is a unique instrument equipped with Microwave Kinetic Inductance Detectors (MKIDS) developed by SRON.

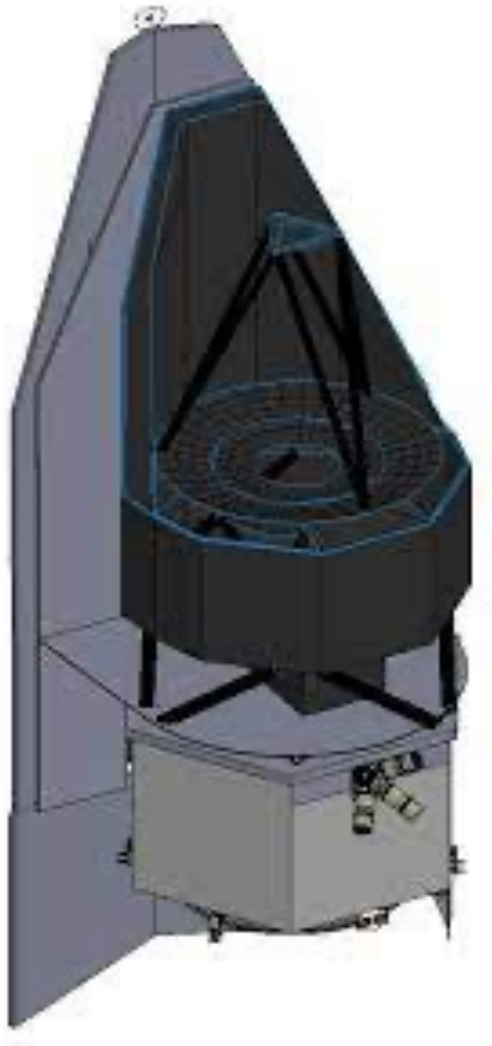

ith two instruments.
carried by JPL and
observing
volved in

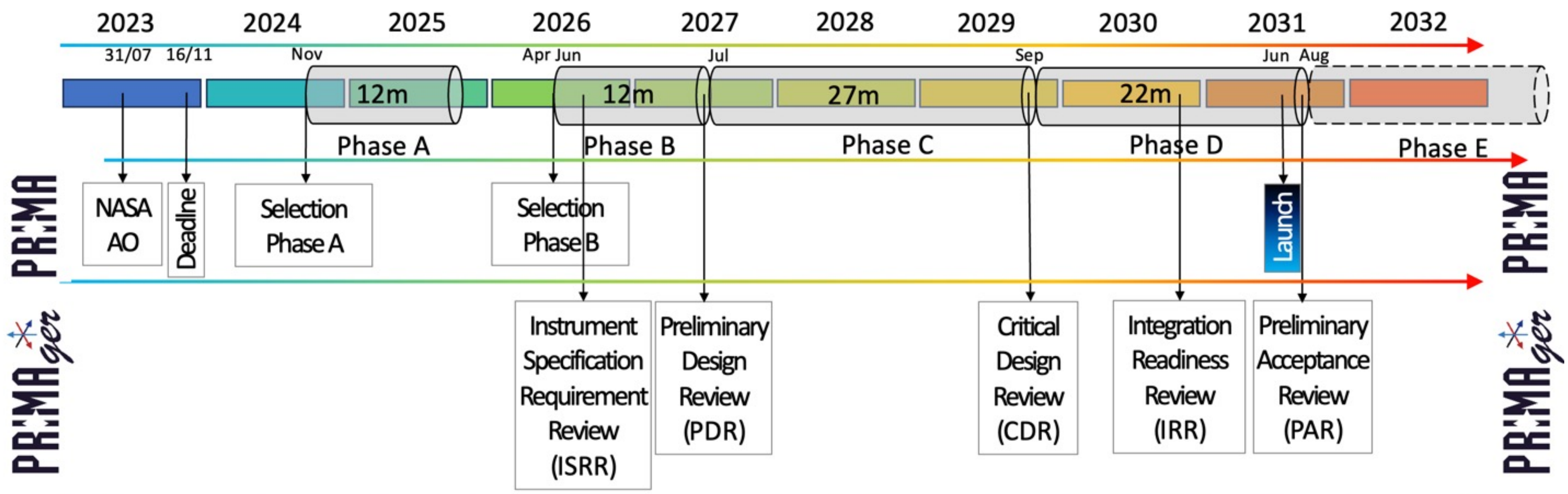

Mass-Metallicity Relation at z ~ 11

Object	z	$M/M_\odot$	Z
s000001	11.4	$(4.96 \pm 3.52)\ 10^8$	0.011 ± 0.004 (continuum + 1 line)
s000010	11.0	$(1.85 \pm 0.66)\ 10^9$	0.007 ± 0.005 (continuum + 1 line)

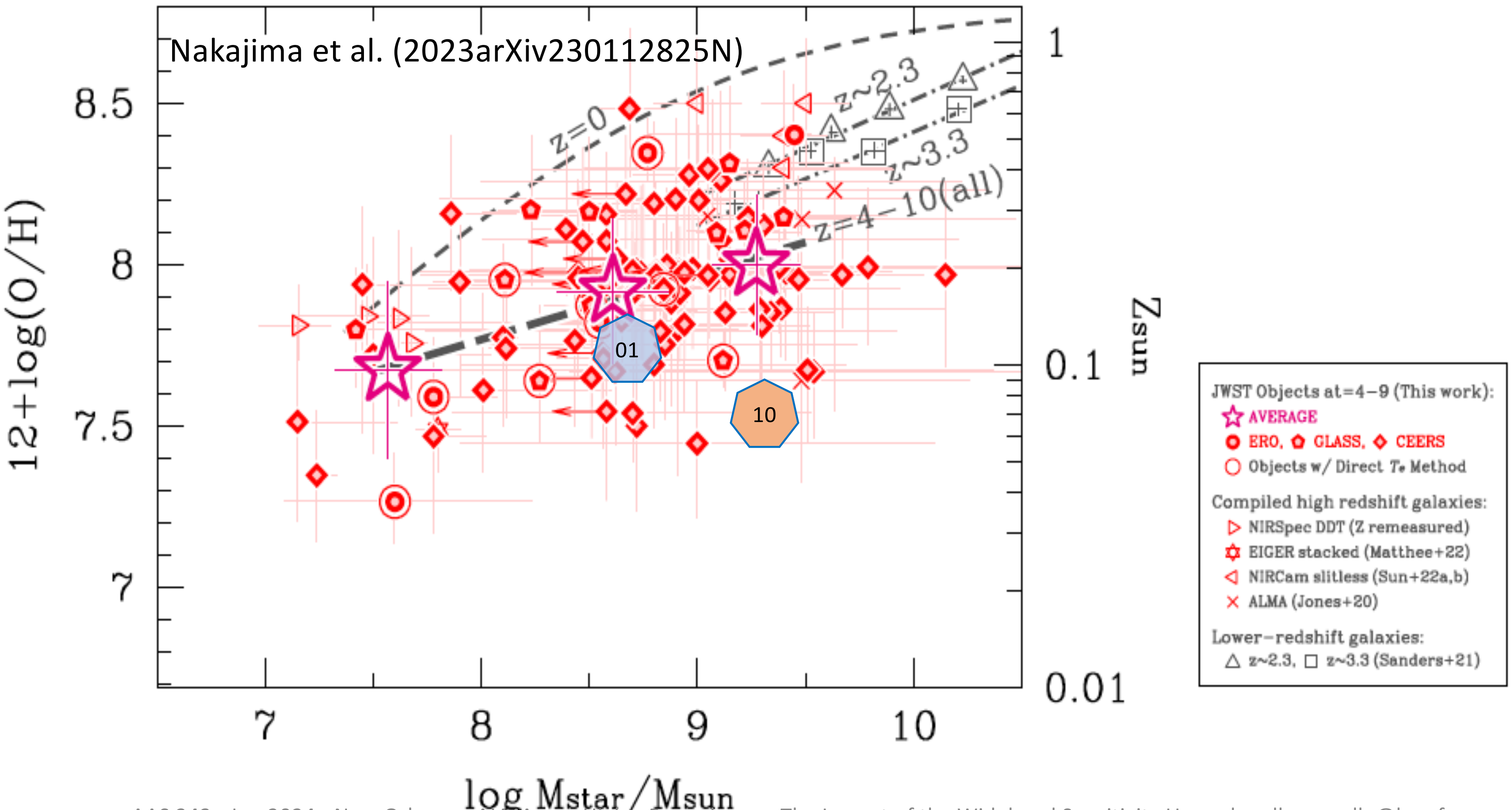

IRAM NOEMA

The NOEMA interferometer is located on the Plateau de Bure at 2550m altitude in the French Alps.

NOEMA antennas can provide **0.2 ″ at 1.3 mm / 230 GHz**

Since 1990, NOEMA is open to the world-wide scientific community, and issues twice a year a call for observing proposals:

- 85% time for partner countries
- 15% observing time for open sky

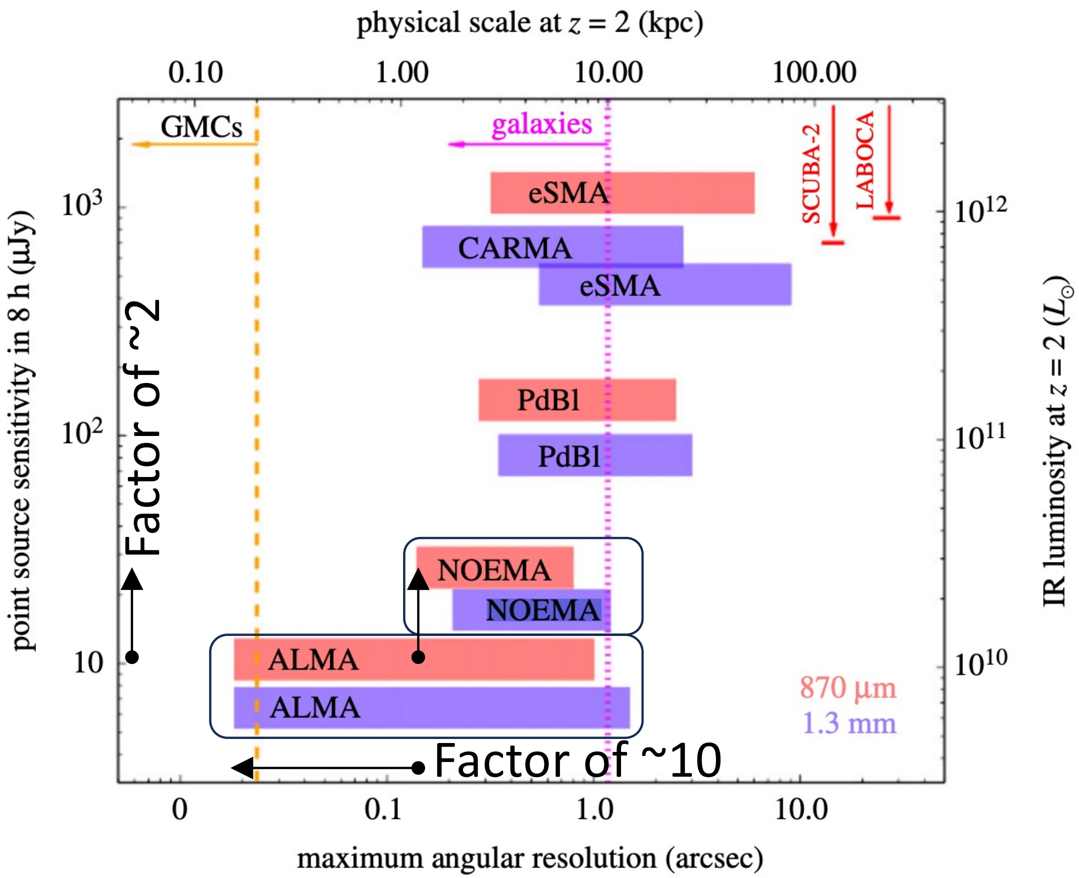

Hodge JA, da Cunha E. 2020
High-redshift star formation in the ALMA array era.
R. Soc. Open Sci. 7: 200556.

DSFG-1: a dusty starburst masquerading as an ultra-high redshift galaxy in JWST CEERS observations

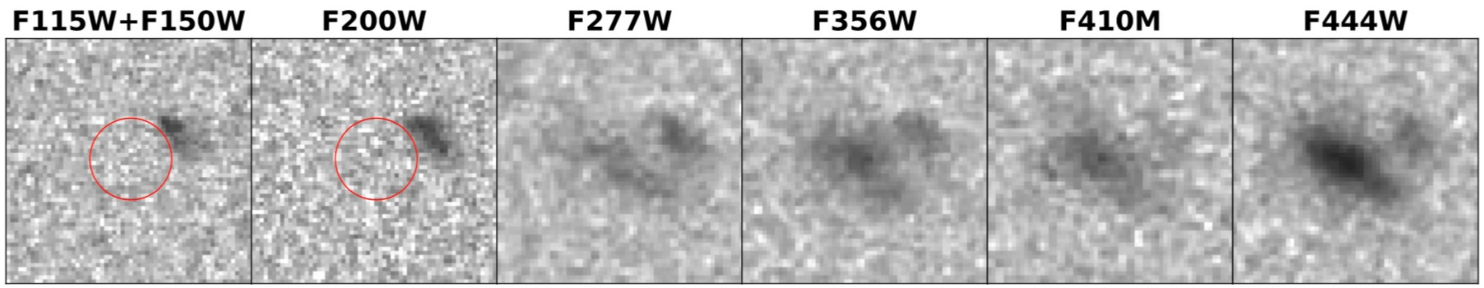

Figure 2. 1.″8×1.″8 cutouts around CEERS-DSFG-1 from the CEERS JWST/NIRCam bands. The source is undetected in F115W, F150W, and F200W (the source's position is indicated with the red circle in the stacked F115W+F150W and F200W images, the dropout bands). The galaxy is well-detected in bluer filters with a red spectral shape. All images follow the same color-code with a maximum value equal to 15× the sky RMS and a minimum value of -1.5σ.

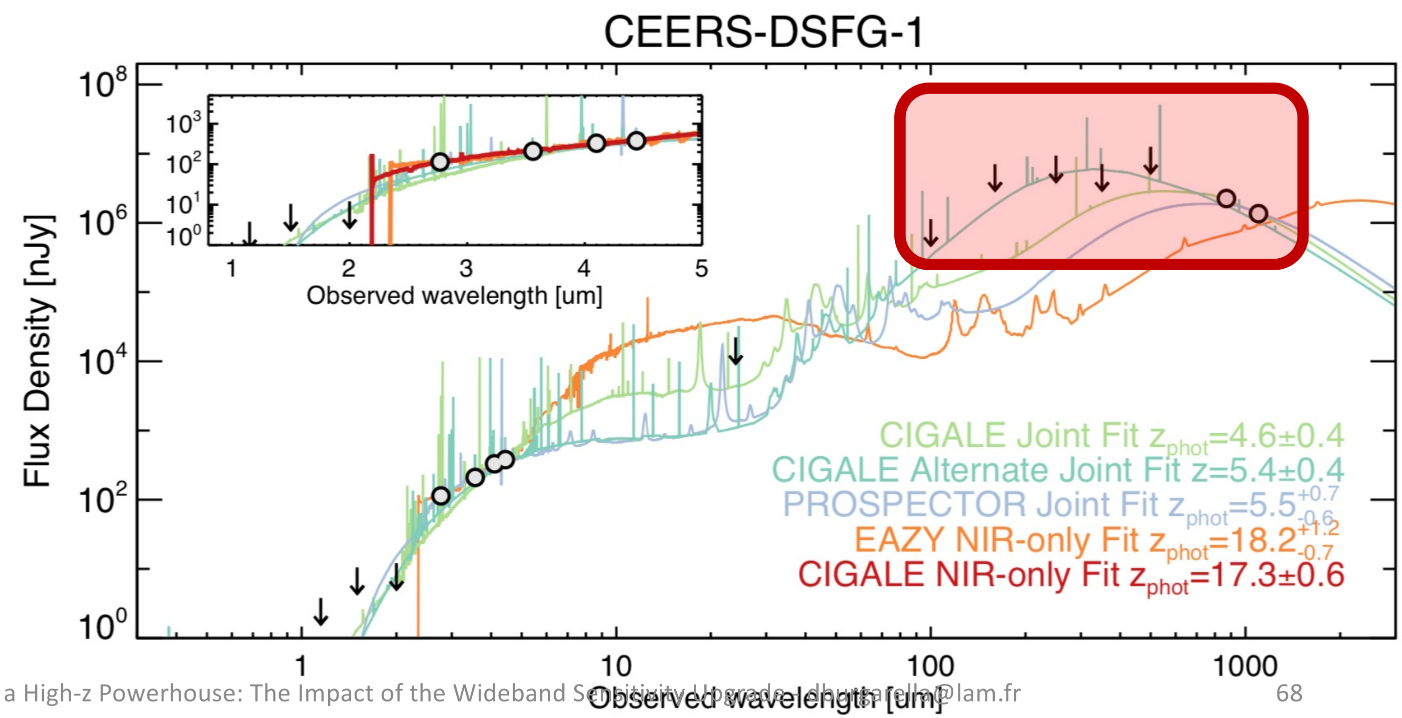


the
FUTURE
is
ours